Applied Energy 350 (2023) 121789

Contents lists available at ScienceDirect

Applied Energy

journal homepage: www.elsevier.com/locate/apenergy

Multi-objective near-optimal necessary conditions for multi-sectoral planning

Antoine Dubois [a,*], Jonathan Dumas [b], Paolo Thiran [c], Gauthier Limpens [c], Damien Ernst [a,d]

[a] Department of Computer Science and Electrical Engineering, Liege University, Liege, Belgium
[b] Research and Development, RTE, Paris, France
[c] Institute of Mechanics, Catholic University of Louvain, Louvain-la-Neuve, Belgium
[d] LTCI, Telecom Paris, Institut Polytechnique de Paris, Paris, France

GRAPHICAL ABSTRACT

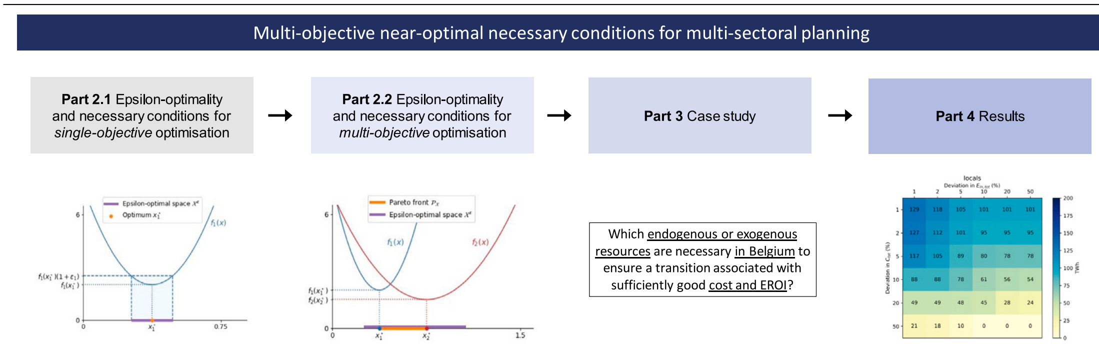

ARTICLE INFO

Dataset link: https://zenodo.org/record/7665340

Keywords:
Energy system modelling
Multi-objective optimisation
Multi-sectoral planning
Near-optimality
Necessary condition
Suboptimal space

ABSTRACT

In the energy transition context, restructuring energy systems and making informed decisions on the optimal energy mix and technologies is crucial. Energy system optimisation models (ESOMs) are commonly used for this purpose. However, their focus on cost minimisation limits their usefulness in addressing other factors like environmental sustainability and social equity. Moreover, by searching for only one global optimum, they overlook diverse alternative solutions. This paper aims to overcome these limitations by exploring near-optimal spaces in multi-objective optimisation problems, providing valuable insights for decision-makers. The authors extend the concepts of epsilon-optimality and necessary conditions to multi-objective problems. They apply this methodology to a case study of the Belgian energy transition in 2035 while considering both cost and energy invested as objectives. The results reveal opportunities to reduce dependence on endogenous resources while requiring substantial reliance on exogenous resources. They demonstrate the versatility of potential exogenous resources and provide insights into objective trade-offs. This paper represents a pioneering application of the proposed methodology to a real-world problem, highlighting the added value of near-optimal solutions in multi-objective optimisation. Future work could address limitations, such as approximating the epsilon-optimal space, investigating parametric uncertainty, and extending the approach to other case studies and objectives, enhancing its applicability in energy system planning and decision-making.

* Corresponding author.
E-mail address: antoine.dubois@uliege.be (A. Dubois).

https://doi.org/10.1016/j.apenergy.2023.121789
Received 1 March 2023; Received in revised form 11 July 2023; Accepted 16 August 2023
Available online 28 August 2023

1. Introduction

The undergoing energy transition requires deep restructuring of energy systems in the long term. The objective is to maintain comparable energy services while replacing fossil fuels with sustainable alternatives. Achieving this goal necessitates significant transformations in the supply chain, conversion processes, and utilisation methods. Energy system planning is required to guide this restructuring and determine the appropriate mix of energy sources and technologies to satisfy a community's or region's future energy demand. The goal of this process is to inform decision-makers to allow them to plan an efficient and sustainable transformation of energy systems. Energy system optimisation models (ESOMs) are commonly preferred in energy system planning [1] due to their ability to explore and analyse multiple design solutions. These models utilise optimisation techniques to explore a wide range of possibilities for the energy system, providing answers to technical questions regarding future challenges.

However, the use of ESOMs often limits the quality of insights they provide, thus reducing their usefulness for decision-makers. Typically, these insights are derived from a single cost-optimal solution, whereas decisions are often made based on various indicators. While cost is a crucial indicator for assessing the affordability and viability of an energy system, focusing solely on this objective can overlook other significant factors, such as environmental sustainability and social equity. Additionally, these insights might not meet the needs of stakeholders with differing interests.

Approaches such as scenario analysis, multi-objective optimisation, and near-optimal space analysis are effective methodologies to surmount the indicated limitation. Scenario analysis enables the indirect integration of objectives by altering the fundamental assumptions underpinning the model. In contrast, multi-objective optimisation directly incorporates these objectives into the model itself. Near-optimal space analysis, the third method, facilitates the inclusion of objectives that cannot be modelled in the decision-making process. In the subsequent sections, we delve into the shortcomings of an overly cost-focused approach. Subsequently, we elucidate these three methodologies, their drawbacks, and the potential advantages of merging multi-objective optimisation with near-optimal space analysis.

1.1. The cost as leading indicator — limits and solutions

ESOMs determine the energy system configurations that minimise or maximise a specified objective. Most studies choose the cost as the objective, and the best configuration is the most cost-effective [1]. This choice is historical, as explained by Pfenninger et al. [2]. Indeed, the first ESOMs (from the MARKAL/TIMES [3] and MESSAGE [4] models) were initially designed for cost minimisation. More recent models followed this trend, such as Dispa-SET, which optimises the operation cost [5]. The study of Yue et al. [6] highlights that by default, ESOMs ignore non-economic factors entering into energy investment decisions and how politics, social norms, and culture shape public policies. This claim is also supported by Pfenninger et al. [2], who specifies that energy system models focus heavily on economic and technical aspects. This focus is inadequate for energy system planning as this problem involves multiple stakeholders with different policy objectives, for whom cost-optimal solutions might not be satisfying. For instance, a model might focus on the cost-effectiveness of integrating wind turbines into a power grid, neglecting diverse stakeholder needs. Governments may prioritise economic growth, environmental bodies aim for carbon reduction, and residents might value landscape preservation. Thus, cost-effective solutions like wind turbines may not align with all stakeholders' varying objectives in energy planning. Moreover, several studies have demonstrated that ignoring non-economic factors increases the uncertainty of the models [2,6]. Fazlollahi et al. [7] also states that, due to uncertainty in some parameters, it is insufficient for energy system sizing to rivet on a unique mono-objective optimal solution. Finally, Trutnevyte [8] shows how cost-optimal scenarios do not adequately represent real-world problems. However, there exist methods for going beyond cost and considering non-economic factors. Some of these methods are presented in the following sections.

1.1.1. Scenario analysis

The first approach to incorporate non-economic factors is scenario analysis. Scenario analysis involves optimising the same model over multiple scenarios with different values for some parameters. Differences between scenarios can result from uncertainties over technological or economic parameters - e.g. future cost of technology. However, they can also stem from political (e.g. nuclear decommissioning) or social considerations (e.g. limitation of onshore wind turbines or transmission lines development). Using scenarios that differ through those considerations allows for studying the effects of non-economic factors. For instance, the study by Fujino et al. [9] compares a fast-growth, technology-oriented scenario to a slow-growth, nature-oriented one. However, as stated in the review of Hughes and Strachan [10], this scenario approach tends to simplify social and political dynamics.

1.1.2. Multi-objective optimisation

A second approach to include non-economic factors is multi-objective optimisation. This approach allows for optimising several objectives simultaneously, highlighting the *trade-offs* that can be obtained. More formally, while different methods exist to apply multi-objective optimisation (e.g. weighted-sum approach, integer cut constraints, ϵ-constraint method, evolutionary algorithm), they exhibit the common goal of obtaining solutions from a Pareto optimal set, also called the *Pareto front*. This Pareto front is composed of *efficient* solutions, i.e. solutions that are at least better than any other solutions in one objective. Thus, it is composed of the set of optimal trade-offs between the studied objectives, i.e. any solution that is not part of the Pareto front is worse in all objectives than at least one solution in the Pareto front. Using multi-objective optimisation, the cost can still be optimised while considering other indicators. For instance, Becerra-López and Golding [11] conducted a study of a Texas power generation system analysing the trade-offs between economic and exergetic costs, i.e. the cumulative exergy – *entropy-free energy* – consumption. They demonstrated how these trade-offs provide insights to the decision-makers by not focusing exclusively on economic cost. Other objectives, such as water consumption, grid dependence on imports or energy system safety, are compared to cost by Fonseca et al. [12,13]. They show how much the assessed criteria impact the design and operation of distributed energy systems. A final example of an alternative objective often combined with the cost is the amount of carbon emissions [14].

1.1.3. Near-optimal spaces analysis

A third methodology that allows taking social and political factors into account is the study of near-optimal spaces, also called sub-optimal or epsilon-optimal spaces. The idea is to analyse solutions close to the optimal solution to understand how the use of resources and technologies varies when allowing a slight deviation in the objective function. This paradigm goes further than multi-objective optimisation, as mentioned by DeCarolis [15]. It allows incorporating unmodelled objectives, typical of social factors, as they are unknown or difficult to model. Indeed, the near-optimal region might contain solutions that are worse in terms of the main objective - e.g. the cost of the system — but better in unmodelled objectives such as risk or social acceptance. This concept was introduced in the 1980s by Brill et al. [16]. The authors proposed the first method for exploring those spaces: the Hop-Skip-Jump method. This algorithm was coined as part of a broader exploration methodology that the authors refer to as Modelling to Generate Alternatives (MGA). This methodology was brought back recently and applied to energy system modelling by DeCarolis [15] and DeCarolis et al. [17]. They led to a renewed interest in such methods.

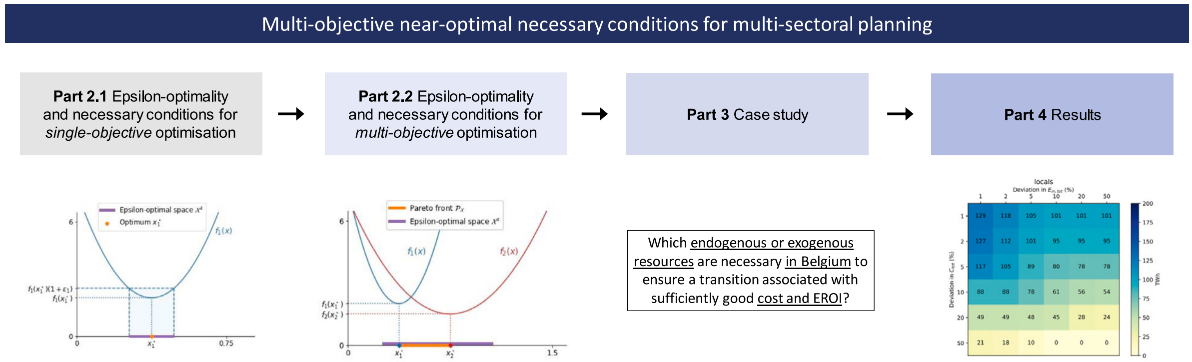

Fig. 1. Graphical abstract showing the structure of the paper. The figures are miniatures of figures located further in the document.

Authors such as Price and Keppo [18] developed new exploration algorithms while Li and Trutnevyte [19] combined MGA with Monte-Carlo exploration to minimise parametric uncertainty.

There are several ways of extracting insights from near-optimal spaces. Most researchers exploring near-optimal spaces focus on computing numerous near-optimal solutions from which they derive insights [18–21]. An alternative approach is to use methods to obtain such insights directly without needing to compute many alternative solutions [22]. The authors of Dubois and Ernst [23] took this approach by introducing the concept of *necessary conditions* for near-optimality, i.e. conditions that are true for every solution in the near-optimal space. For instance, this can provide insights into the required capacity in a given technology to retain a certain level of system cost-effectiveness. More specifically, Dubois and Ernst [23] showed how, for instance, at least 200 GW of new offshore wind need to be installed Europe-wise to stay within 10% of the cost optimum.

1.2. Research gaps, scientific contributions and organisation

The exploration of near-optimal spaces has been used in mono-objective optimisation problems but not, according to the author's best knowledge, in multi-objective optimisation problems. However, these methods could also be valuable in multi-objective optimisation setups. Indeed, while modelling and integrating more objectives, multi-objective optimisation still leaves aside some unmodelled objectives. Analysing solutions in the near-optimal space of multi-objective optimisation problems is a method to address this issue.

This paper thus aims to fill this gap by:

1. extending the concepts related to near-optimal spaces to multi-objective optimisation;
2. computing necessary conditions in a multi-objective context to highlight the range of insights that can be derived from them.

The first point is addressed in Section 2 by first introducing the mathematical concepts of near-optimality and necessary conditions in a single-objective framework (see Section 2.1) and then extending them to multi-objective optimisation (see Section 2.2). Section 3 then translates those concepts to a real case study: the multi-sectoral expansion of the Belgian energy system. The results of this case study, including necessary conditions representing the necessary amount of different energy resources, are presented in Section 4 before highlighting the contributions of this paper in Section 5. We can already highlight one of those contributions: the open-source release of the code [24] and the data [25] used to achieve this study. The graphical representation of the organisation of this paper is depicted in Fig. 1.

2. Problem statement

In this section, the methodological contribution is described. It is illustrated in a mathematical form to enhance its universality. Indeed, this method could be applied to other problems than ESOM. It will be applied in Section 3 to an ESOM formulation to facilitate understanding of this method.

The first part of this section introduces the concepts of epsilon-optimal space and necessary conditions for single-objective optimisation [23]. The second part extends these concepts to multi-objective optimisation by:

1. generalising the optimisation problem to multiple objectives,
2. presenting generic notions related to multi-objective optimisation, including the image of the feasible space, efficient solutions, and the Pareto front, and
3. explaining the extension of the concepts of epsilon-optimality and necessary conditions to multi-objective optimisation.

2.1. Single-objective optimisation

2.1.1. Optimisation problem and epsilon-optimality

Let $\mathcal{X}$ be a feasible space and $f : \mathcal{X} \rightarrow \mathbb{R}_+$ an objective function in the positive reals. The single-objective optimisation problem is

$$\min_{x \in \mathcal{X}} f(x) \quad . \tag{1}$$

Let $x^\star$ denote an optimal solution to this problem that is: $x^\star \in \arg\min_{x\in\mathcal{X}} f(x)$.

Definition 1. An ϵ**-optimal space**, with $\epsilon \geq 0$, is defined as follows

$$\mathcal{X}^\epsilon = \left\{ x \in \mathcal{X} \mid f(x) \leq (1+\epsilon) f(x^\star) \right\} \quad . \tag{2}$$

Comment: The ϵ-optimal space is the set of the feasible solutions $x \in \mathcal{X}$ with objective value $f(x)$ no greater than $(1+\epsilon)f(x^\star)$. The deviation from the optimal objective value is measured via ϵ, called the *suboptimality coefficient*. Fig. 2 illustrates those concepts. A note must be made on the specific case $f(x^\star) = 0$. In this case, $\mathcal{X}^\epsilon$ resumes to $\arg\min_{x\in\mathcal{X}} f(x)$, making the analysis of near-optimal spaces trivial.

2.1.2. Necessary conditions

The concepts of *condition*, *necessary condition*, and *non-implied necessary condition* introduced in this section allow determining features which are common to all solutions in a given ϵ-optimal space. We illustrate each definition using an example.

Definition 2. A **condition** is a function $\phi : \mathcal{X} \rightarrow \{0, 1\}$. A set of conditions is denoted Φ.

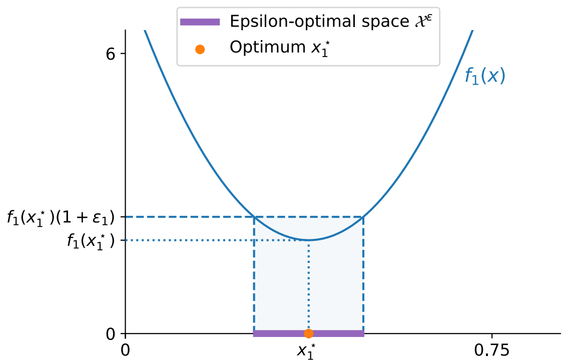

Fig. 2. Graphical representation of an ϵ-optimal space of a mono-objective optimisation problem in $\mathcal{X} = \mathbb{R}_+$. The function f_1 that is minimised is shown in blue. Its minimum is located at $x_1^\star$. Using this value and its corresponding objective value $f_1(x_1^*)$ allows to determine an ϵ-optimal space $\mathcal{X}^\epsilon$ with $\epsilon = \epsilon_1$. The values of the different parameters and functions used in this example are described in Appendix A.

Example. Let the feasible space $\mathcal{X}$ be the set of reals, i.e. $\mathcal{X} = \mathbb{R}$, then, the set of conditions $\boldsymbol{\Phi}$ could be the set of conditions of the form $\phi_c(x) := x \geq c$ with $x \in \mathcal{X}$ (thus $x \in \mathbb{R}$) and $c \in \mathbb{R}$.

Definition 3. A **necessary condition** for ϵ-optimality is a condition which is true for any solutions in $\mathcal{X}^\epsilon$. For a feasible space $\mathcal{X}$, set of conditions $\boldsymbol{\Phi}$ and suboptimality coefficient ϵ, $\phi \in \boldsymbol{\Phi}$ is a necessary condition if

$$\forall x \in \mathcal{X}^\epsilon : \phi(x) = 1 \quad . \tag{3}$$

The set of all necessary conditions for ϵ-optimality in $\boldsymbol{\Phi}$ is denoted $\boldsymbol{\Phi}^{\mathcal{X}^\epsilon}$.

Example. Let us consider that the epsilon-optimal space is given by $\mathcal{X}^\epsilon = [0, 1]$. Then, the condition $\phi_0(x) := x \geq 0$ is respected by all $x \in \mathcal{X}^\epsilon$, making ϕ_0 a necessary condition. Moreover, it is straightforward to show that the set of all conditions in $\boldsymbol{\Phi}$ which are necessary is $\boldsymbol{\Phi}^{\mathcal{X}^\epsilon} = \{\phi_c \mid c \leq 0\}$. Indeed, any condition $\phi_c(x) := x \geq c$ is true over $\mathcal{X}^\epsilon = [0, 1]$ if $c \leq 0$.

As shown in Dubois and Ernst [23], necessary conditions can provide insights into features common to many near-optimal solutions. However, depending on how conditions are defined, their study also claims the number of necessary conditions can be infinite, which is counterproductive in providing insights. This situation happens, for instance, in our previous example. Indeed, the set $\boldsymbol{\Phi}^{\mathcal{X}^\epsilon} = \{\phi_c \mid c \leq 0\}$ contains an infinite number of necessary conditions. To limit the number of conditions, we introduce the concept of *non-implied necessary conditions*.

Definition 4. A **non-implied necessary condition** for ϵ-optimality is a necessary condition $\phi \in \boldsymbol{\Phi}^{\mathcal{X}^\epsilon}$ that is not implied by any other necessary condition $\phi' \in \boldsymbol{\Phi}^{\mathcal{X}^\epsilon} \setminus \{\phi\}$, where $\boldsymbol{\Phi}^{\mathcal{X}^\epsilon}$ is the set of necessary conditions for ϵ-optimality. The set of non-implied necessary conditions is denoted $\overline{\boldsymbol{\Phi}}^{\mathcal{X}^\epsilon}$.

Example. In our example, the only non-implied necessary condition is ϕ_0, *i.e.* $\overline{\boldsymbol{\Phi}}^{\mathcal{X}^\epsilon} = \{\phi_0\}$. The set of necessary conditions is $\boldsymbol{\Phi}^{\mathcal{X}^\epsilon} = \{\phi_c \mid c \leq 0\}$. In this set, ϕ_0 implies all other conditions and is not implied by any of them. Indeed, for any x, knowing that $x \geq 0$ is true implies that $x \geq c$ when $c \leq 0$. Thus, knowing that ϕ_0 is a necessary condition implies that any ϕ_c with $c \leq 0$ is a necessary condition, whatever the ϵ-optimal space. On the opposite, it is not possible to imply that ϕ_0 is a necessary condition from the knowledge of other necessary conditions in the set $\boldsymbol{\Phi}^{\mathcal{X}^\epsilon} = \{\phi_c \mid c \leq 0\}$. This defines ϕ_0 as a *non-implied* necessary condition.

The interested reader can find a more formal definition of implication leading to alternative definitions of non-implied necessary conditions in Appendix B.

2.1.3. Non-implied necessary condition computation

This section presents the detailed computation of a particular type of non-implied necessary condition to provide a practical sense of these concepts. It demonstrates how to compute a non-implied necessary condition from a set of conditions taking the form of constrained sums of variables. In the case studies described in Section 3, this type of condition is used to study the minimum amount of energy that can be driven from different sources.

Let $\mathcal{X} \subset \mathbb{R}^n$ be a feasible space, $f : \mathcal{X} \to \mathbb{R}_+$ an objective function to minimise over this space, and $\boldsymbol{\Phi}_{\mathbf{d}}$ a set of conditions defined as follows:

$$\boldsymbol{\Phi}_{\mathbf{d}} = \left\{ \phi^c_{\mathbf{d}}(\mathbf{x}) = \mathbf{d}^T\mathbf{x} \geq c \right\} \quad , \tag{4}$$

where $\mathbf{x} \in \mathcal{X}$, $\mathbf{d} \in \{0,1\}^n$ and $c \in \mathbb{R}$. The conditions are constrained sums of variables $\mathbf{d}^T\mathbf{x} = \sum_{i=1}^n d_i x_i$. In this particular case, Dubois and Ernst [23] have proven that $\phi^{c^\star}_{\mathbf{d}} = \mathbf{d}^T\mathbf{x} \geq c^*$ with $c^* = \min_{\mathbf{x}\in\mathcal{X}^\epsilon} \mathbf{d}^T\mathbf{x}$ is the only non-implied necessary condition that can be derived from $\boldsymbol{\Phi}_{\mathbf{d}}$. The value c^* represents the minimum value that $\mathbf{d}^T\mathbf{x}$ can take over the set $\mathcal{X}^\epsilon$, that is when allowing a deviation of ϵ from the optimal value $f(\mathbf{x}^\star)$. Algorithm 1 illustrates the computation of this value in three steps.

Algorithm 1: Computation of a non-implied necessary condition - Single-objective case

Data:
- f - objective function,
- $\mathcal{X}$ - feasible space,
- ϵ - suboptimality coefficient,
- $\mathbf{d}$ - binary vector defining the conditions $\mathbf{d}^T\mathbf{x}$

Result: c^*

Steps:
1. Solve $\min_{\mathbf{x}\in\mathcal{X}} f(\mathbf{x})$ to obtain $\mathbf{x}^\star$.
2. Build $\mathcal{X}^\epsilon$ by adding the constraint $f(\mathbf{x}) \leq (1+\epsilon) f(\mathbf{x}^\star)$ to $\mathcal{X}$.
3. Solve $c^* = \min_{\mathbf{x}\in\mathcal{X}^\epsilon} \mathbf{d}^T\mathbf{x}$.

Example. Let us illustrate this algorithm on the travellings salesman problem. This problem aims to find the shortest possible route a salesman can take to visit a set of cities exactly once and return to the starting city. Mathematically, we can model this problem in the following way. Let $G = (V, E)$ be a complete undirected graph, where $V = \{1, 2, \dots, n\}$ is the set of cities, and E is the set of edges connecting the cities. Each edge $e = (i, j)$ has a non-negative weight $w(e)$ representing the distance between city i and city j. Let x_{ij} be a binary decision variable equal to 1 if the salesman travels directly from city i to city j in the tour and 0 otherwise. The objective is to minimise the total distance travelled by the salesman, i.e.: $\min \sum_{(i,j)\in E} w_{ij} x_{ij}$. This objective must be met under a series of constraints we will not detail here. Let us assume now that there are two types of routes: paved and gravel. The salesman wants to avoid taking gravel routes while maintaining a path that is not much longer than the optimal path. This new path can be obtained using Algorithm 1. Step 1 consists in solving the original problem. Using the optimal solution of this problem, one can perform step 2 by adding the constraint $f(\mathbf{x}) \leq (1+\epsilon) f(\mathbf{x}^\star)$ to the initial problem. In this constraint, $\mathbf{x}$ is a vector containing all x_{ij}, $f(\mathbf{x}) = \sum_{(i,j)\in E} w_{ij} x_{ij}$, and $\mathbf{x}^\star$ is the optimal solution. The value of ϵ can vary depending on the relative increase in path length the salesman is willing to accept. The third step can then be performed by setting an appropriate $\mathbf{d}$. As the salesman wants to minimise the number of gravel routes travelled, all values of $\mathbf{d}$ corresponding to this type of route are set to 1. The value c^* obtained as the optimal value of this third step gives the minimal number of routes that must be taken to ensure that the total length of the path travelled does not deviate by more than ϵ of the optimal length.

2.2. Multi-objective optimisation

This section extends the concepts presented previously to multi-objective optimisation while introducing notions specific to this type of optimisation problem.

2.2.1. Problem formulation

Let $\mathbf{f} := (f_1, \dots, f_k, \dots, f_n)$ be a vector of n objective functions such that $\forall k\ f_k : \mathcal{X} \to \mathbb{R}_+$. We seek to minimise these functions over the feasible space $\mathcal{X}$, which, using the notation of Ehrgott [26], we note:

$$\text{“}\min_{x\in\mathcal{X}}\text{”} \quad \mathbf{f}(x) \quad . \tag{5}$$

Let $\mathcal{Y}$ be the image of $\mathcal{X}$ in the objective space:

$$\mathcal{Y} = \mathbf{f}(\mathcal{X}) = \{y \in \mathbb{R}^n \mid y = \mathbf{f}(x) \text{ for some } x \in \mathcal{X}\} \quad . \tag{6}$$

This space is the image of $\mathcal{X}$ under the objective functions $\mathbf{f}$, and $\mathbf{f}(x) := (f_1(x), \dots, f_k(x), \dots, f_n(x))$. Therefore, $\mathcal{Y} \in \mathbb{R}^n_+$ and each of its components y_k are defined by $y_k = f_k(x)$ for some $x \in \mathcal{X}$.

2.2.2. Efficient solutions and Pareto front

A way to highlight compromises between the objectives $(f_1, \dots, f_k, \dots, f_n)$ is to compute efficient (or Pareto optimal) solutions. As defined by Ehrgott [26]:

Definition 5. A feasible solution $\hat{x} \in \mathcal{X}$ is called **efficient** when there is no other $x \in \mathcal{X}$ such that $\forall k\ f_k(x) \le f_k(\hat{x})$ and $f_i(x) < f_i(\hat{x})$ for some i, that is, no other $x \in \mathcal{X}$ has a smaller or equal value in all objectives $(f_1, \dots, f_k, \dots, f_n)$ than $\hat{x}$.

According to Ehrgott [26], multiple denominations exist for the set of efficient points. This paper uses 'Pareto front' to indiscriminately name the set of efficient points or their image in the objective space.

Definition 6. A **Pareto front** $\mathcal{P}_\mathcal{X}$ is the set

$$\mathcal{P}_\mathcal{X} = \Big\{ \hat{x} \in \mathcal{X} \mid \nexists x \in \mathcal{X}, \quad \forall k\ f_k(x) \le f_k(\hat{x}), \exists i\ f_i(x) < f_i(\hat{x}) \Big\} . \tag{7}$$

In the objective space, a Pareto front is defined as:

$$\mathcal{P}_\mathcal{Y} = \Big\{ \hat{y} \in \mathcal{Y} \mid \nexists y \in \mathcal{Y}, \quad \forall k\ y_k \le \hat{y}_k, \exists i\ y_i < \hat{y}_i \Big\} \quad . \tag{8}$$

A Pareto front can be composed of an infinity of points. Thus, it is typical to compute a subset of the efficient solutions which compose it. This set is named *approximated Pareto front*. It is denoted by $\mathcal{P}_{\mathcal{X},m}$ (or equivalently $\mathcal{P}_{\mathcal{Y},m}$) where m is the number of points in the approximation.

Definition 7. An **approximate Pareto front** $\mathcal{P}_{\mathcal{X},m}$, with $m \in \mathbb{N}$, is a subset of m efficient solutions in the Pareto front $\mathcal{P}_\mathcal{X}$.

Several techniques exist to obtain those efficient solutions, the two most famous being the '*weighted-sum approach*' and the '*ϵ-constraint method*' [26]. The weighted-sum approach consists of solving:

$$\min_{x\in\mathcal{X}} \sum_{k=1}^{n} \lambda_k f_k(x) \quad \forall k\ \lambda_k > 0 \quad . \tag{9}$$

The ϵ-constraint method resolves in solving:

$$\begin{aligned} &\min_{x\in\mathcal{X}}\ f_j(x) \\ &\text{s.t. } f_k(x) \le \epsilon_k \text{ for } k = 1, \dots, n \text{ and } k \ne j \quad , \end{aligned} \tag{10}$$

where $\forall k\ \epsilon_k \in \mathbb{R}$.

2.2.3. Multi-criteria epsilon-optimal spaces

Starting from a Pareto front $\mathcal{P}_\mathcal{X}$, it is possible to define an ϵ-optimal space, given a *suboptimality coefficients vector* of deviations in each objective: $\boldsymbol{\epsilon} = (\epsilon_1, \dots, \epsilon_k, \dots, \epsilon_n) \in \mathbb{R}^n_+$. This space is denoted by $\mathcal{X}^\epsilon$ in the decision space and $\mathcal{Y}^\epsilon$ in the objective space.

In the mono-objective setup, the ϵ-optimal space is defined as the set of points $x \in \mathcal{X}$ whose objective value $f(x)$ do not deviate by more than an ϵ fraction from the optimal objective value, i.e. $f(x) \le (1+\epsilon) f(x^\star)$. In a multi-objective case, there is no optimum but a set of efficient points composing the Pareto front. This leads us to define the ϵ-optimal space as follows:

Definition 8. In a multi-objective optimisation problem, the **$\boldsymbol{\epsilon}$-optimal space** $\mathcal{X}^\epsilon$, with $\boldsymbol{\epsilon} = (\epsilon_1, \dots, \epsilon_k, \dots, \epsilon_n) \in \mathbb{R}^n_+$, is the set of points x whose objective values $f_k(x)$ do not deviate by more than an ϵ_k fraction from the objective values $f_k(\hat{x})$ of *at least one* solution $\hat{x}$ of the Pareto front $\mathcal{P}_\mathcal{X}$ for all k. It is the space

$$\mathcal{X}^\epsilon = \Big\{ x \in \mathcal{X} \mid \exists \hat{x} \in \mathcal{P}_\mathcal{X}, \quad \forall k\ f_k(x) \le (1+\epsilon_k) f_k(\hat{x}) \Big\} \quad . \tag{11}$$

Alternatively, this space can be defined as:

$$\mathcal{X}^\epsilon = \bigcup_{\hat{x}\in\mathcal{P}_\mathcal{X}} \Big\{ x \in \mathcal{X} \mid \forall k\ f_k(x) \le (1+\epsilon_k) f_k(\hat{x}) \Big\} \quad . \tag{12}$$

Fig. 3 depicts a graphical representation of an ϵ-optimal space in a multi-objective framework and how it is built from efficient solutions.

Definition (11) relies on the entire Pareto front. However, practically, only a subset $\mathcal{P}_{\mathcal{X},m}$ of m efficient points of the Pareto front is computed and used to obtain an approximation of the ϵ-optimal space, denoted $\mathcal{X}^\epsilon_m$.

Definition 9. An approximation $\mathcal{X}^\epsilon_m$, with $m \in \mathbb{N}$, of an ϵ-optimal space $\mathcal{X}^\epsilon$ is the space

$$\mathcal{X}^\epsilon_m = \Big\{ x \in \mathcal{X} \mid \exists \hat{x} \in \mathcal{P}_{\mathcal{X},m}, \quad \forall k\ f_k(x) \le (1+\epsilon_k) f_k(\hat{x}) \Big\} \quad . \tag{13}$$

Alternatively, this space can be defined as:

$$\mathcal{X}^\epsilon_m = \bigcup_{\hat{x}\in\mathcal{P}_{\mathcal{X},m}} \Big\{ x \in \mathcal{X} \mid \forall k\ f_k(x) \le (1+\epsilon_k) f_k(\hat{x}) \Big\} \quad . \tag{14}$$

The alternative formulation defines $\mathcal{X}^\epsilon_m$ as a union of spaces, where each space is the set of points whose objective value in each f_k does not deviate by more than an ϵ_k fraction from the objective values $f_k(\hat{x})$ of one solution $\hat{x}$ in the approximated Pareto front $\mathcal{P}_{\mathcal{X},m}$. Fig. 4 shows three examples of approximate ϵ-optimal spaces $\mathcal{X}^\epsilon_m$ in the objective space (therefore noted $\mathcal{Y}^\epsilon_m$) using three approximated Pareto fronts $\mathcal{P}_{\mathcal{Y},m}$, with different numbers and spread of efficient solutions.

2.2.4. Necessary conditions

In the multi-objective optimisation framework, necessary conditions and non-implied necessary conditions for ϵ-optimality can be defined in the same manner as in the one-dimensional setting (see Definitions 3 and 4, respectively). The only difference stems from the replacement of $\mathcal{X}^\epsilon$ by $\mathcal{X}^\epsilon$.

2.2.5. Non-implied necessary condition computation

The computation of a non-implied necessary condition from conditions of type $\mathbf{d}^T\mathbf{x} \ge c$ presented in Section 2.1.3 is generalised to the multi-criteria case. In the mono-objective case, it was sufficient to minimise the sum $\mathbf{d}^T\mathbf{x}$ over $\mathcal{X}^\epsilon$ to obtain the value c^* corresponding to the non-implied necessary condition $\mathbf{d}^T\mathbf{x} \ge c^*$. However, in a multi-objective setup, we do not have access to $\mathcal{X}^\epsilon$ but to its approximation

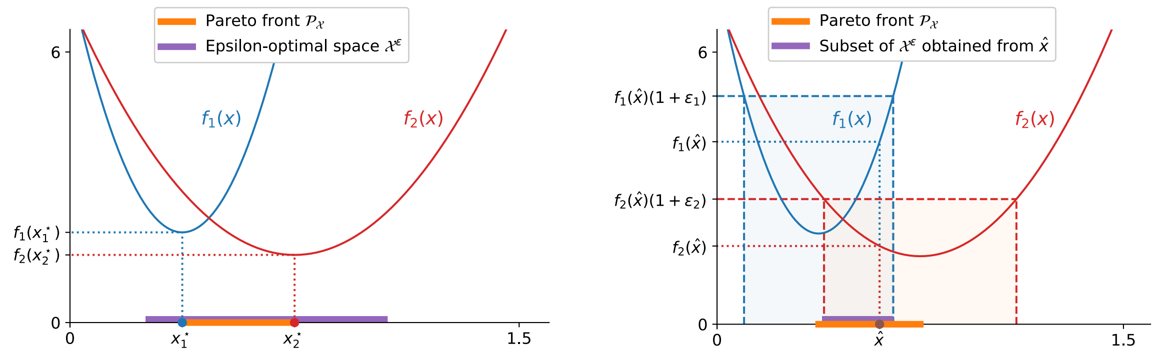

(a) Full representation of $\mathcal{X}^{\epsilon}$

(b) Computation of a subset of $\mathcal{X}^{\epsilon}$ from a single point $\hat{x}$ of the Pareto front $\mathcal{P}_{\mathcal{X}}$

Fig. 3. Graphical representation of an ϵ-optimal space of a multi-objective optimisation problem in $\mathcal{X} = \mathbb{R}_+$. The two functions to be minimised f_1 and f_2 are represented in blue and red, respectively, and their respective minimums are $x_1^\star$ and $x_2^\star$. The Pareto front $\mathcal{P}_{\mathcal{X}}$ containing all efficient solutions is represented in orange. Fig. 3(a) shows in purple the full ϵ-optimal space $\mathcal{X}^{\epsilon}$ for a suboptimality coefficient vector $\epsilon = (\epsilon_1, \epsilon_2)$. As shown in Eq. (12), this space is the union of sub-spaces that can be computed from efficient solutions. Fig. 3(b) shows how one of these subspaces, corresponding to the efficient solution $\hat{x}$, can be computed. From the value $\hat{x}$, the corresponding objective values $f_1(\hat{x})$ and $f_2(\hat{x})$ are obtained. This allows to determine all the solutions in $\mathcal{X}$ whose objective value is smaller than $f_k(\hat{x})(1+\epsilon_k)$ for $k \in 1, 2$. The values of the different parameters and functions used in this example are described in Appendix A.

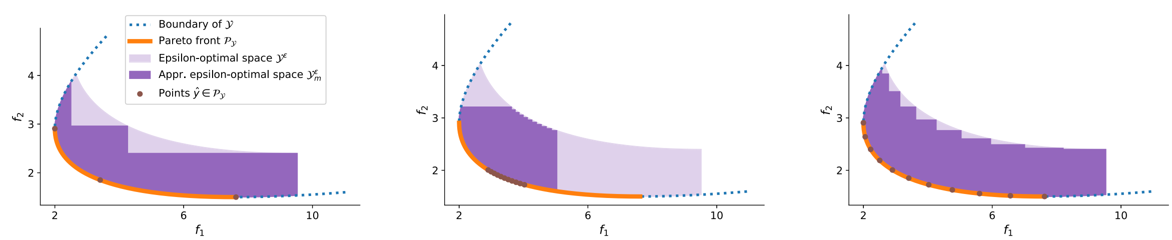

(a) Few well-spread points

(b) Numerous badly-spread points

(c) Numerous well-spread points

Fig. 4. Graphical representations in the objective space of approximations $\mathcal{Y}^{\epsilon}_m$ of an ϵ-optimal space of a multi-objective optimisation problem based on three different approximate Pareto front $\mathcal{P}_{\mathcal{Y},m}$. The axes correspond to the two functions to minimise, i.e. f_1 and f_2. The boundary of the image of the feasible space $\mathcal{Y}$ is represented in blue in the three cases. The part of this boundary corresponding to the entire Pareto front $\mathcal{P}_{\mathcal{Y}}$ is drawn in orange. The complete ϵ-optimal space $\mathcal{Y}^{\epsilon}$ corresponding to this Pareto front is coloured in light purple. Each graph corresponds to a different approximate Pareto front $\mathcal{P}_{\mathcal{Y},m}$. These sets of points are represented in brown. From each of these points, part of the approximate ϵ-optimal spaces can be computed, and their union is represented in solid purple. The values of the different parameters and functions used in this example are described in Appendix A.

$\mathcal{X}^{\epsilon}_m$, which is the union of several subsets, each corresponding to one point in $\mathcal{P}_{\mathcal{X},m}$ (i.e. a subset of the Pareto front). The minimum over this space can thus be obtained by taking the minimum of the minima of $\mathbf{d}^T\mathbf{x}$ over each of these subsets. Even with this approach, $\mathcal{X}^{\epsilon}_m$ being a subset of $\mathcal{X}^{\epsilon}$, minimising $\mathbf{d}^T\mathbf{x}$ over it will only provide an upper bound $\tilde{c}$ of the value c^*, i.e. $\tilde{c} \geq c^*$. Algorithm 2 shows how this value can be obtained.

Algorithm 2: Computation of a non-implied necessary condition - Multi-objective case

Data:
- $\mathcal{X} \in \mathbb{R}^n$ - feasible space,
- $\mathbf{f}$ - objective functions,
- m - number of points,
- ϵ - vector of suboptimality coefficients,
- $\mathbf{d}$ - binary vector defining the conditions $\mathbf{d}^T\mathbf{x}$

Result: $\tilde{c}$

Steps:
1. Draw m points $\hat{\mathbf{x}}^{(1)}, \dots \hat{\mathbf{x}}^{(i)}, \dots \hat{\mathbf{x}}^{(m)}$ of the Pareto front using an appropriate method.
2. For all $i \in [1, 2, \dots, m]$, compute $c^{(i)} = \min \mathbf{d}^T\mathbf{x}$ over the space $\{\mathbf{x} \in \mathcal{X} \mid \forall k \; f_k(\mathbf{x}) \leq (1+\epsilon_k) f_k(\hat{\mathbf{x}}^{(i)})\}$.
3. Take the minimum $\tilde{c} = \min_{i \in [1,2,\dots,m]} c^{(i)}$ of these values to find the appropriate condition $\phi_{\tilde{c}}$.

There is no guarantee that the condition $\mathbf{d}^T\mathbf{x} \geq \tilde{c}$ is a (non-implied) necessary condition. Indeed, it could be the case that for a solution $\mathbf{x} \in \mathcal{X}^{\epsilon} \backslash \mathcal{X}^{\epsilon}_m$ that $\mathbf{d}^T\mathbf{x} < \tilde{c}$. To make the upper bound $\tilde{c}$ as close as possible to the real minimal value c^*, one must reduce the size of the difference $\mathcal{X}^{\epsilon} \setminus \mathcal{X}^{\epsilon}_m$. Minding this gap can be done by improving the number and spread of efficient solutions in the approximated Pareto front. As defined by Alarcon-Rodriguez et al. [27], solutions with a good spread can be seen as having good coverage of the actual Pareto front. The three graphs of Fig. 4 show visually how, by increasing the number and the spread of efficient solutions drawn from the Pareto front, the approximated ϵ-optimal space covers a more significant subset of the points of the entire ϵ-optimal space.

Example. Let us continue with the travelling salesman problem introduced in Section 2.1.3. We introduce a new set of non-negative weights $t(e)$ representing the time needed to travel between city i and j. We now have two objectives: the total distance travelled $f(\mathbf{x}) = \sum_{(i,j)\in E} w_{ij} x_{ij}$ and the total time travelled $g(\mathbf{x}) = \sum_{(i,j)\in E} t_{ij} x_{ij}$ to visit all cities. Minimising these two objectives might lead to different solutions. We can use appropriate techniques to determine efficient solutions $\hat{\mathbf{x}}$ from the Pareto front, expressing the trade-offs between these two objectives. If the salesman is still interested in avoiding the gravel routes while maintaining close-to-optimal length and time of travel, we can employ Algorithm 2. For a fixed set of suboptimality coefficients, step 2 implies adding two constraints to the initial problem and minimising $\mathbf{d}^T\mathbf{x}$ for each efficient solution. As in the mono-objective case, the only values of **d** set to 1 are the ones corresponding to gravel routes. Finally, step 3 will give us a value $\tilde{c}$, which expresses an upper bound on the minimum number of gravel routes the salesman needs to take to avoid deviations in time and length larger than ϵ_1 and ϵ_2.

3. Case study

In this section, a case study using an ESOM will illustrate the concepts and methodology presented in the previous section. First, the context of the case study and the question to which it tries to provide an answer are presented. The modelling tool used to implement the methodology is then introduced, and its main features are detailed. Finally, each element introduced in Section 2 is specified to the case study.

3.1. Context

In the European Green Deal [28], the European Commission raised the European Union's ambition to reduce GHG emissions to at least 55% below 1990 levels by 2030. Then by 2050, Europe aims to become the world's first carbon-neutral continent. Europe still relies massively on fossil fuels to satisfy its energy consumption (~75% coming from coal, natural gas and oil according to the International Energy Agency [29]) as well as non-energy usages (e.g. chemical feed-stocks, lubricants and asphalt for road construction [30]). The use of these fuels is the primary source of GHG emissions. Carbon-neutral sources of energy must thus be developed to curb emissions. The possibilities are numerous, and one of the coming decade's main challenges will be deciding which resources to invest in. Several criteria will motivate these choices.

The most common criterion for discriminating between options is cost. Indeed, as highlighted by Pfenninger et al. [2] and DeCarolis [15], most studies use the cost indicator to plan the energy transition. This choice makes sense as the cost of investment, maintenance and operation of the energy system impacts the final consumers' energy bill. Thus, minimising the system cost is a social imperative to allow every citizen access to affordable energy.

A lesser-known indicator, encompassing technical and social challenges, is the system's *energy return on investment* (EROI). When defined system-wise, the EROI is a ratio that measures the usable energy delivered by the system (E_{out}) over the amount of energy required to obtain this energy (E_{in}) [31]. When the amount of energy required to deliver a given energy service increases, the EROI of the system decreases. In some sense, EROI measures the ease with which energy is extracted to transform it into a form that benefits society. There are various manners of defining E_{in} and E_{out}, and incidentally, the EROI of a system. These definitions depend mainly on what parts of the *energy cascade* - as presented in Brockway et al. [32] or Dumas et al. [33] - are considered. This paper considers that invested energy E_{in} encompasses the energy used to build the system infrastructure, 'from the cradle to the grave', and to operate this system. Following the methodology of Dumas et al. [33], E_{out} will correspond to the final energy consumption (FEC) of the system, as defined in the European Commission [34] standard. FEC is the total energy, measured in TWh, consumed by end-users. It encompasses the energy directly used by the consumer and excludes the energy used by the energy sector, e.g. deliveries and transformation.

While cost and EROI can be linked (e.g. the transport of energy resources will increase both the system cost and invested energy), they are not fully correlated and favouring one or the other can lead to different system configurations, as illustrated later in Section 4. Both criteria can be included in the decision process by modelling them as objectives in optimisation problems. These objectives can be optimised individually or co-optimised using multi-criteria optimisation techniques. In this case study, we will show how, using these objectives in the methodology presented in Section 2, the following question can be addressed:

> Which resources are necessary to ensure a transition associated with sufficiently good **cost and EROI**?

Indeed, the answer to this question can be obtained by computing necessary conditions corresponding to the minimum amount of energy that needs to come from these resources.

This question is, however, relatively broad, and for the sake of conciseness, it needs to be specified. On top of decision criteria, considerations such as energy independence (enhanced with the Russian invasion of Ukraine) and social acceptance (e.g. the 'not-in-my-backyard' phenomena) are paramount in planning the energy transition. These considerations will impact the type of resources that will be exploited. Indeed, the first consideration incentives a push for domestically produced energy, while the latter favours the opposite. The first tends to minimise the amount of exogenous resources in the system, while the latter minimises the amount of energy coming from endogenous resources. To consider these elements, the previous question can be refined to:

> **Which endogenous or exogenous resources are necessary** to ensure a transition associated with sufficiently good cost and EROI?

This study focuses on one of the European countries: Belgium. Belgium made the same commitments for 2030 and 2050 as the European Union [35]. Thus, it faces the challenge of replacing its fossil-based economy with carbon-free solutions while striking the right balance between endogenous and exogenous resources. Belgium's population density exacerbates this challenge. In 2019, Belgium had the second-highest population density in Europe (excluding Malta) with 377 people per km^2, behind the Netherlands (507 people per km^2) [36]. The available land for onshore energy development is thus limited, while offshore production is limited to around 8 GW of wind potential [37]. Other domestic resources such as solar, biomass, waste, or hydro also have limited potential. This situation entails a small local energy potential compared to its demand. The study Limpens et al. [38] evaluates that available local Belgian resources can only cover 42% of the country's primary energy consumption. This situation strongly impacts the type of resources Belgium must rely on.

Therefore, the question that will be addressed in this case study is:

> Which endogenous or exogenous resources are necessary **in Belgium** to ensure a transition associated with sufficiently good cost and EROI?

3.2. EnergyScope TD

To answer this question, an appropriate ESOM is needed. The commitments set for 2035 and 2050 cover all sectors of the economy, not just electricity production. To achieve net zero ambitions, carbon-neutral solutions must be implemented for electricity, heat, mobility, and non-energy. These different sectors can be modelled using an open-source whole-energy system model such as EnergyScope TD (ESTD) [39].

ESTD can be categorised as an ESOM. According to Contino et al. [40], ESTD is a *whole-energy* system model, i.e. a model that captures the different energy sectors exhaustively. Moreover, ESTD optimises the energy system with an hourly resolution and has the advantage of having a simple mathematical formulation compared to other models [39]. Using optimisation techniques, it determines the investment decisions and sizing of various technologies (e.g. wind turbines, gas power plants, boilers) as well as the selection of resources (e.g. wind, gas, diesel) required to meet different types of end-use demand (EUD) listed in Appendix C; and the hourly operation of the system. Mathematically, ESTD models the energy system as a linear programming problem. It takes a series of parameters as input and outputs the values of investment and operational variables determined by minimising an objective while respecting a series of constraints. The objective is a linear function; constraints are linear equalities or inequalities.

Parameters and variables can be indexed temporally. The default temporal horizon T is one year with an hourly resolution. To reduce the computational burden of the optimisation, the horizon is clustered by selecting a number of typical days, 12 by default. Thus, time-dependent parameters and variables are indexed by a typical day td and an hour h. The only exception is storage technologies, whose energy levels are computed over all the hours of the year t to allow storage longer than a day up to seasonal. The equivalence between the original hourly-resolution temporal horizon and the typical days is done via a time-indexed set $THTD(t)$ associating each hour t of the year with a corresponding couple $(td,h) = THTD(t)$. This set is essential to understand some of the equations in the rest of this section.

ESTD has been extensively used and validated in the Belgian case [33,38,41–44]. More specifically, in Limpens et al. [38], the authors studied the 2035 Belgian energy system using ESTD and built the corresponding data set. This year is a trade-off between a long-term horizon where policies can still be implemented and a horizon short enough to define the future of society with a group of known technologies. To build on these resources, we will model the Belgian energy system for 2035.

To finish this section, it is essential to note that while the results presented in this paper are valid for Belgium, they could easily be extended to other countries. Indeed, ESTD has already been used to model the energy systems of other countries such as Switzerland [45,46] and Italy [47]. Moreover, adapting those models to implement the methodology presented in this paper only requires minor modifications, as presented in the following sections.

3.3. Feasible space

In the initial optimisation problem

$$\text{“}\min_{x\in\mathcal{X}}\text{”} \quad \mathbf{f}(x) \quad , \tag{15}$$

the first element to define is the feasible space $\mathcal{X}$ over which the optimisation is performed. This study modelled the feasible space using ESTD as a linear programming problem. Therefore, the problem to solve has the following form:

$$\begin{aligned} &\text{“}\min_{\mathbf{x}}\text{”} \quad \mathbf{f}(\mathbf{x}) \\ &\quad s.t. \quad A\mathbf{x} \geq \mathbf{b} \quad , \end{aligned} \tag{16}$$

where $\mathbf{x}$ is the vector of variables of the problem, while A and $\mathbf{b}$ are a matrix and vector of parameters, respectively. More information on the specific variables, parameters and constraints used in ESTD can be found in Limpens et al. [39] and the model's documentation [48].

3.3.1. Constraint on GHG emissions

A constraint that is of particular interest given the context of this case study is the limit on GHG emissions, i.e.

$$GWP_{tot} \leq 35 \text{ [MtCO}_2\text{-eq/y]} \quad . \tag{17}$$

In this section, we briefly describe how this constraint is defined. The total yearly GHG emissions of the system are computed using a life-cycle analysis (LCA) approach. Thus, they include the GHG emissions along the whole life cycle, i.e. 'from the cradle to the grave' of the technologies and resources considered in ESTD. In ESTD, the global warming potential (GWP) expressed in $MtCO_2$-eq./year is used as an indicator to aggregate emissions of different GHG. Then, the yearly emissions of the system, which are denoted GWP_{tot}, are defined as follows:

$$GWP_{tot} = \sum_{j\in TECH} \frac{GWP_{constr}(j)}{lifetime(j)} + \sum_{i\in RES} GWP_{op}(i) \quad , \tag{18}$$

where $TECH$ and RES are the sets of technologies and resources modelled in ESTD. GWP_{constr} represents the GWP for the construction of a technology, while GWP_{op} gives the GWP linked to the operation of a resource. More specifically, $GWP_{constr}(j)$ is the GWP of technology j over its entire lifetime allocated to one year based on the technology lifetime $lifetime(j)$. $GWP_{op}(i)$ is the GWP related to the use of resource i over one year.

The 35 $MtCO_2$-eq/y limit chosen in this case study comes from the following reasoning. According to the International Energy Agency (IEA), Belgium's 1990 territorial GHG emissions were approximately 105 $MtCO_2$-eq [29]. Thus, the targets of the European Green Deal imply reaching 47 $MtCO_2$-eq/y in 2030 and 0 $MtCO_2$-eq/y in 2050.[1] By conducting a linear interpolation between these dates, the 2035 Belgian GHG emissions should reach approximately 35 $MtCO_2$-eq/y. This target is used as a hard constraint for GWP_{tot} in the model: $GWP_{tot} \leq 35$ [$MtCO_2$-eq/y].

3.4. Objectives

The second step in formalising the problem consists in choosing appropriate objectives. As mentioned at the start of this section, our interest lies in solutions with a sufficiently good cost and EROI. This choice implies optimising the system by minimising cost and maximising EROI. To better match the methodology presented in Section 2 where functions are minimised, E_{in} (i.e. the energy invested in the system) will be used as objective instead of EROI (the equivalence is detailed in the following). The following sections define precisely the two objectives used in the case study.

3.4.1. System cost

The first objective is the total annual cost of the system, $f_1 = C_{tot}$, defined as:

$$C_{tot} = \sum_{j\in TECH} \left(\tau(j)C_{inv}(j) + C_{maint}(j)\right) + \sum_{i\in RES} C_{op}(i) \quad . \tag{19}$$

The yearly system cost is the sum of $\tau(j)C_{inv}(j)$, the annualised investment cost of each technology with C_{inv} the total investment cost and τ the annualisation factor, $C_{maint}(j)$, the operating and maintenance cost of each technology and $C_{op}(i)$, the operating cost of the resources. This last variable is equal to

$$C_{op}(i) = \sum_{t\in T|\{h,td\}\in THTD(t)} c_{op}(i)\mathbf{F}_t(i,h,td) \quad , \tag{20}$$

where $c_{op}(i)$ is the cost of resource i in [€/MWh] and $\mathbf{F}_t(i,h,td)$ corresponds to the use in [MWh] of resource i at time (h,td). The values of $c_{op}(i)$ for each resource used in the study case are given in Tables 1 and 2. The study of Limpens et al. [39] or the online documentation [48] provides more detail on this indicator.[2]

3.4.2. Energy invested in the system

The second objective f_2 is E_{in}, the energy invested in the system over one year:

$$E_{in} = \sum_{j\in TECH} \frac{E_{constr}(j)}{lifetime(j)} + \sum_{i\in RES} E_{op}(i) \quad , \tag{21}$$

with $E_{constr}(j)$, the energy invested to built technology j, annualised by dividing it by its lifetime, and $E_{op}(i)$ the energy to operate, i.e. produce,

[1] Practically, the 2050 target is to be climate neutral, meaning the GHG emission can be greater than 0 but must be compensated by carbon capture.

[2] In the mathematical formulation of the model, an additional factor $t_{op}(h,td)$ is added to Eqs. (20), (22), and (26). This parameter is set to 1 in the implementation of the model used in this case study. It is thus removed from equations for clarity.

Table 1
2035 values of c_{op}, cost of the resource [€/MWh], and e_{op}, energy invested in obtaining 1 MWh of the resource [MWh/MWh], for each resource. Most values for c_{op} come from [48]. Data for e_{op} relies on [49], using the *ecoinvent* database [50], and on [51]. Abbreviations: Renewable (Re.), Electricity (Elec.).

	c_{op} [€/MWh]	e_{op} [MWh/MWh]
Endogenous resources		
Hydro	0	0
Solar	0	0
Waste	23.1	0.0577
Wet biomass	5.76	0.0559
Wind	0	0
Wood	32.8	0.0491
Exogenous resources		
Ammonia	76.0	[a]0.174
Ammonia (Re.)	81.8	[a]0.295
Diesel	79.7	0.210
Bio-diesel	120	[a]0.101
Elec. import	84.3	0.123
Gas	44.3	0.0608
Gas (Re.)	118	[a]0.147
Gasoline	82.4	0.281
Bio-ethanol	111	[a]0.101
H2	87.5	0.083
H2 (Re.)	119	[a]0.134
LFO	60.2	0.204
Methanol	82.0	0.0798
Methanol (Re.)	111	[a]0.146

[a]The values are based on the work by Orban [51].

and transport resource i over one year. Similarly to the cost indicator, this last variable is equal to

$$E_{op}(i) = \sum_{t\in T|\{h,td\}\in THTD(t)} e_{op}(i)\mathbf{F}_t(i,h,td) \quad , \tag{22}$$

where $e_{op}(i)$ is the energy invested (in [MWh/MWh]) to obtain one MWh of the resource i. The values of $e_{op}(i)$ for each resource used in the study case are given in Tables 1 and 2. More detail is provided by Dumas et al. [33] (in which E_{in} is referred to as $E_{in,tot}$).

Minimising E_{in} would be equivalent to maximising EROI, i.e. E_{out}/E_{in}, if E_{out}, which in our case is the FEC, was constant. It is not the case in ESTD. In this model, only the values for the EUD, presented in Table C.5, are fixed. While EUD measures an energy service, FEC measures the quantity of energy used to deliver this service. FEC is thus always measured in [TWh], while the unit for EUD will depend on the demand. For instance, the EUD for heat will be measured in [TWh] while [Mt-km] will be used for mobility. Using technology-dependent conversion factors, FEC can be converted into EUD and vice-versa. For instance, in ESTD, a FEC of 1 kWh of electricity supplies an EUD of 5.8 passenger-km with a battery-electric car. As the conversion factors depend on the installed technologies, which depend on the optimisation results, FEC is an output of the ESTD model and is not constant. Nonetheless, the constant EUD cannot be employed directly as E_{out} to compute the EROI, as it is an energy service, not an amount of energy. Therefore, the FEC is used to compute E_{out} and, incidentally, the EROI of the system.

3.5. Pareto front

Once all the elements of the initial optimisation problem (5) are set up, one can compute efficient solutions from the Pareto front using one of the methods described in Section 2.2.2. This case study uses a modified version of the ϵ-constraint method. It is applied by minimising E_{in} over the feasible space with the additional constraint $C_{tot} \leq \epsilon(1 + C^{\star}_{tot})$ where $\epsilon \in \mathbb{R}_+$ and $C^{\star}_{tot}$ is the cost-optimal value, i.e. solving

$$\begin{aligned} &\min_{x\in\mathcal{X}} \ E_{in} \\ &\text{s.t. } C_{tot} \leq (1+\epsilon)C^{\star}_{tot} \end{aligned} \tag{23}$$

Table 2
Estimated cost c^{*}_{op} [€/MWh] and estimated energy invested in obtaining 1 MWh of the resource e^{*}_{op} [MWh/MWh] for hydro, solar and wind. The estimation is done by computing the total cost at the C_{tot} optimum and invested energy at the E_{in} optimum of the technologies that use these resources (i.e. PV for solar, onshore and offshore wind for wind and hydro river for hydro) and then dividing it by the total energy used from these resources at the corresponding optimums, indicated in Table 4.

	c^{*}_{op} [€/MWh]	e^{*}_{op} [MWh/MWh]
Hydro	53.7	0.0489
Solar	50.0	0.147
Wind	47.0	0.0350

This method is a slight modification of the method described in Eq. (10) where ϵ is a relative rather than absolute value. It has the benefit of defining the constraint proportionally to the optimal value in the associated objective and thus be directly interpretable. For instance, if the optimal cost is 75 B€, one would use ϵ values of 1, 5, and 10% instead of absolute values of 75.75, 78.75 and 82.5 B€. To obtain several points over the Pareto front, the method was repeated for different values of ϵ in $]0, C^{e}_{tot}/C^{\star}_{tot}[$ where C^{e}_{tot} is the value of C_{tot} at the E_{in} optimum and $C^{\star}_{tot}$ is the cost optimum.

3.6. Near-optimal spaces

The efficient solutions are used to define approximate near-optimal spaces $\mathcal{X}^{\epsilon}_{m}$, with $\epsilon = (\epsilon_{C_{tot}}, \epsilon_{E_{in}})$ following Eq. (14) of Definition 9. They are unions of spaces defined around unique, efficient solutions, $\hat{x} \in \mathcal{P}_{\mathcal{X},m}$. Each space can be easily defined by adding to the original ESTD model the two linear constraints, which are:

$$C_{tot}(x) \leq (1+\epsilon_{C_{tot}})C_{tot}(\hat{x}) \quad , \tag{24}$$

$$E_{in}(x) \leq (1+\epsilon_{E_{in}})E_{in}(\hat{x}) \quad . \tag{25}$$

3.7. Necessary conditions

The last concept to define is the type of necessary conditions computed in the case study. We are interested in the necessary resources for a transition with a sufficiently low cost and invested energy. We will thus compute the necessary conditions corresponding to the minimum amount of energy that needs to come from a specific individual or group of resources. Mathematically, the set of such conditions would be:

$$\Phi_{\overline{RES}} = \left\{ \sum_{\substack{i\in\overline{RES},\\ t\in T|\{h,td\}\in THTD(t)}} \mathbf{F}_t(i,h,td) \geq c \right\} \quad , \tag{26}$$

where $\overline{RES} \subseteq RES$ is a set of resources, $\mathbf{F}_t(i,h,td)$ the use of resource i at time (h,td) and $c \in \mathbb{R}_+$. $\overline{RES}$ can contain any resource. However, in the context presented in Section 3.1, we have highlighted a particular interest in two groups of resources: endogenous and exogenous. We will focus primarily on those two sets and give a more detailed description of their resources. In ESTD, endogenous resources (noted RES_{endo}) include wood, wet biomass, waste, wind, solar, hydro, and geothermal energy. Exogenous resources (noted RES_{exo}) are the other resources in the model: ammonia, renewable ammonia, imported electricity, methanol, renewable methanol, hydrogen, renewable hydrogen, coal, gas, renewable gas, light fuel oil, gasoline, diesel, biodiesel, and bioethanol. Renewable fuels such as renewable ammonia, methanol, and gas are assumed to be produced from renewable electricity. Tables 1 and 2 list the model's resources and the associated input parameters required to compute the cost and invested energy when employing them.

Table 3
Values of C_{tot} and E_{in} objectives at the optimums.

	C_{tot} optimum	E_{in} optimum
C_{tot} [B€/y]	**52.8**	56.8
E_{in} [TWh/y]	74.0	**61.0**

Table 4
Amount of energy used from each endogenous and exogenous resource at C_{tot} and E_{in} optimums. The last column shows the maximum potential of each resource. Some potentials are directly fixed as parameters. The others are computed from the maximum capacity and capacity factors of the technologies using these resources.

Energy [TWh/y]	C_{tot} optimum	E_{in} optimum	Max. potential
Endogenous	**185**	**164**	**185**
Hydro	0.469	0.486	[a]0.488
Solar	61.5	54.2	[a]61.6
Waste	17.8	4.12	17.8
Wet biomass	38.9	38.9	38.9
Wind	42.6	43.0	[a]43.0
Wood	23.4	23.4	23.4
Exogenous	**202**	**211**	∞
Ammonia (Re.)	65.6	0	∞
Bio-diesel	0	3.14	∞
Elec. import	27.6	27.6	27.6
Gas	28.2	34.5	∞
Gas (Re.)	4.98	48.5	∞
H2 (Re.)	19.4	44.8	∞
Methanol (Re.)	56.4	52.8	∞
Total	**387**	**375**	∞

[a]Potential computed from maximum capacity and capacity factors.

4. Results

In this section, we provide the answer to the question that was asked at the beginning of Section 3:

> Which endogenous or exogenous resources are necessary in Belgium to ensure a transition associated with sufficiently good cost and EROI?

This answer is obtained by computing necessary conditions corresponding to the minimum amount of energy coming from specific resources required to ensure ϵ-optimality in C_{tot} and E_{in}. However, before diving into the necessary conditions, we first analyse how the system is configured at the two optimums and show the differences between those configurations. Then, by analysing efficient solutions, we determine how this system evolves when trade-offs are made between C_{tot} and E_{in}. Finally, knowing the Pareto front, we compute ϵ-optimal spaces and necessary conditions corresponding to the minimum amount of energy coming from different resources in Belgium. The description of the algorithm used to compute those necessary conditions can be found in Appendix D.

4.1. Analysis of the system configuration at the two optimums

The Belgian energy system is analysed when optimising C_{tot} and E_{in} individually, with a maximum carbon budget GWP_{tot} of 35 MtCO$_2$-eq/y. To set a baseline to which we can compare the necessary conditions computed in the following sections, we analyse the amount of endogenous and exogenous resources used at each optimum. Table 3 shows the value of the two objective functions at the two optimums and Table 4 details which energy sources are used in the system.

4.1.1. Results at the cost optimum

The optimal cost $C^{\star}_{tot}$ is equal to 52.8 B€/y. At this optimum, the total amount of primary energy used in the system is 387 TWh/y, 48% of which comes from endogenous resources and the rest from exogenous resources.

For endogenous resources, the values for wet biomass, waste and wood are equal to their maximum potentials — set as input model parameters. This observation makes sense as the c_{op} of these resources in Table 1 indicate they are among the cheapest. The hydro, solar and wind energy quantities are also very close to their maximum potential. For these resources, the maximum is not set directly on the quantity of energy but on the capacities of the technologies using these resources. For instance, the model can install a maximum of 6 GW of offshore wind turbines and 10 GW of onshore wind turbines, which are the two technologies using wind as a resource. These maximum capacities can then be multiplied by the capacity factors of the corresponding technologies to obtain a maximum energy potential. Moreover, these resources are considered free in terms of cost and invested energy, as shown in Table 1. The cost of using them arises from the technologies to extract them from the environment. Table 2 shows approximated values for c_{op} and e_{op}. They are computed by dividing the cost or energy invested for building and maintaining the technologies using them by the total energy used from these resources — shown in Table 4. These approximated values show that hydro, solar and wind are among the cheapest resources, which explains their extensive use.

The model has no maximum potential for exogenous resources except for imported electricity. This potential is reached as, even though c_{op} is relatively high for imported electricity, it does not require any conversion technology to produce the final electricity demand. Some 65.6 TWh/y of renewable ammonia is used in the system, 55.4 TWh/y of which is used for electricity production and low-temperature heat generation, while the remaining 10.2 TWh/y is used to satisfy non-energy demand. Most renewable methanol is used to produce high-value chemicals, even though 3.6 TWh/y of this resource is used for fuelling boat freight. Finally, gas (renewable or not) is used to produce heat and electricity and fuel buses for public mobility.

4.1.2. Results at the invested energy optimum

The optimal energy invested $E^{\star}_{in}$ amounts to 61 TWh/y. Among the 375 TWh/y of primary energy in the system, 164 TWh/y (44%) come from endogenous resources and 211 TWh/y (56%) from exogenous resources. A series of resources, including wet biomass, wood, wind, hydro and imported electricity, are used at or near their maximum potential. This is not the case for waste and solar. In particular, for solar, e_{op} is about three times higher than any other endogenous resource. This result can be explained by the higher energy needed to build 1 GW of PV combined with a low average capacity factor compared to hydro river plants or wind turbines. Some electricity is produced using natural and renewable gas, while ammonia for non-energy demand is produced from H2 using the Haber-Bosch process. The remaining amount of gas is used to produce heat. Finally, high-value chemicals are produced using renewable methanol, while 3.14 TWh/y of bio-diesel is used for boat freight.

4.1.3. Comparison

Table 3 shows how the two objective functions vary from one optimum to the other. The increase in cost when optimising E_{in} is limited to 7.67%. Invested energy at the C_{tot} optimum is around 74 TWh/y, representing an increase of more than 20% from the E_{in} optimal value.

As shown in Table 4, the total amount of energy needed in the system differs only by 3%, but there are some differences between the two energy mixes. At the C_{tot} optimum, the energy coming from endogenous resources is 21 TWh/y higher, while energy from exogenous resources is 9 TWh/y smaller. At each optimum, the share of endogenous resources in the energy mix (48% and 44%, respectively) is close to the maximum of 42% primary energy coming from endogenous

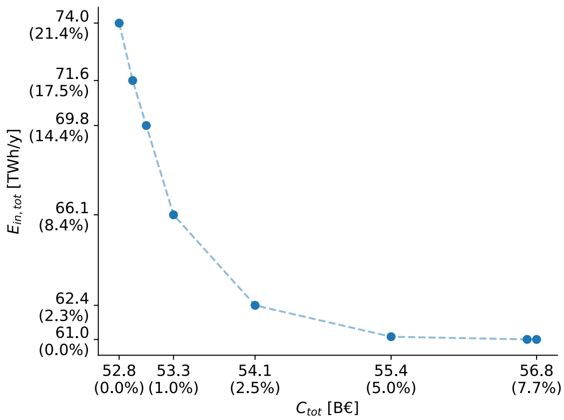

Fig. 5. Approximated Pareto front showing trade-offs between C_{tot} and E_{in}. On the axis, the absolute values of C_{tot} and E_{in} are shown and completed, in parenthesis, by the deviations from the optimal objective values in each objective. For instance, for C_{tot}, the value $C_{tot}/C^{\star}_{tot} - 1$ is shown in parenthesis.

resources computed by Limpens et al. [38]. These values confirm the substantial dependence of Belgium on imported resources to supply its energy consumption.

Looking at individual resources, solar and renewable ammonia, used to produce electricity when optimising C_{tot}, are replaced by fossil and renewable gas at the E_{in} optimum. At this optimum, a percentage of the total 80 TWh/y of gas is used to produce high-temperature heat instead of waste. The additional 35.4 TWh/y of renewable hydrogen is used for three things: ammonia production (which is directly imported when optimising cost), combined heat and electricity production, and public mobility. Finally, while boat freight is fuelled using renewable methanol at the C_{tot} optimum, bio-diesel is preferred at the E_{in} optimum.

4.2. Pareto front

Fig. 5 shows the values of C_{tot} and E_{in} at the efficient solutions obtained using the method described in Section 3.5 for values of ϵ equal to 0.25, 0.5, 1.0, 2.5, 5.0 and 7.5%. The two additional points at the curve extremes correspond to each objective's optimum. The axes are labelled both in terms of the absolute values of the objective functions but also – in parenthesis – in terms of the deviations of these values from the optimal objective value, i.e. $C_{tot}/C^{\star}_{tot} - 1$ and $E_{in}/E^{\star}_{in} - 1$.

This graph shows that E_{in} decreases quite rapidly, saving 10 TWh/y out of 74 TWh/y (∼−14%) when increasing C_{tot} by a relatively small amount of 2.5%. This behaviour can also be interpreted as: choosing the optimal cost implies a considerable addition in invested energy. Inversely, as already mentioned, C_{tot} is still relatively low at the E_{in} optimum, i.e. it only increases by 7.5%.

Fig. 6 shows the amount of endogenous and exogenous resources used at each efficient solution, starting on the left with the cost optimum and moving towards the invested energy optimum on the right. As stated when comparing optimums, there is only a minor change for endogenous resources when going from one optimum to the other. This change, the reduction of solar and waste energy, appears when allowing a 5% deviation in cost.

More change is happening for exogenous resources (Fig. 6(b)). As we increase cost and decrease the invested energy, ammonia is gradually replaced by gas (both natural and renewable). At a 2.5% cost increase, the amount of renewable H2 starts increasing. Ammonia is wholly removed from the system at 5%, while natural gas use reaches its maximum and starts to decline. The same happens for renewable ammonia when reaching a 7.5% cost increase, and some bio-diesel appears. Overall, the change in the total amount of exogenous resources used is non-monotonic. Starting to decrease, it then increases when reaching the 5% threshold, corresponding to the drop in endogenous resources use.

4.3. Necessary conditions

Analysing efficient solutions gives a first appreciation of the variety of system configurations, offering a trade-off between different objectives. However, using the necessary conditions, we can go one step further by providing features respected by all those solutions and some slightly less efficient solutions. We use Algorithm 2 to compute non-implied necessary conditions stemming from different sets of conditions of the type defined by (26) in Section 3.7. The main parameter defining these conditions is $\overline{RES}$, the set of resources over which the constrained sum is computed. The output of this algorithm is a value $\tilde{c}$, which defines a non-implied necessary condition for this set of resources. Practically, this value represents the minimum amount of energy that needs to come from this set of resources to ensure that C_{tot} and E_{in} do not deviate by more than an ϵ fraction from at least one solution in the Pareto front. We will first compute this $\tilde{c}$ value for conditions defined using the set of endogenous and the set of exogenous resources. We will then look at sets containing one individual resource.

4.3.1. Endogenous vs. exogenous resources

In this first section, we compare the values $\tilde{c}$ of non-implied necessary conditions computed from the sets $\Phi_{RES_{endo}}$ and $\Phi_{RES_{exo}}$. These conditions are computed for different values of deviations ϵ. In this case, the tuples $\epsilon = (\epsilon_{C_{tot}}, \epsilon_{E_{in}})$ corresponds to all the possible combinations of 1, 2, 5, 10, 20, and 50%.

Comparing Figs. 7(a) and 7(b) shows that the behaviours of the minima in endogenous and exogenous resources are very different. For endogenous resources, the minimum for deviations of 1% in both objectives is already down to 130 TWh/y, representing a 42% and 26% decrease from the C_{tot} and E_{in} optima, respectively. This amount is divided by more than two when the deviation reaches 10% in both objectives, leaving only 60 TWh/y left from endogenous resources. The $\tilde{c}$ value then reaches 0 TWh/y when allowing an increase of 50% in C_{tot}. These results show that energy from endogenous resources can be reduced by a significant amount for reasonably low increases in cost and invested energy.

For exogenous resources, there is little to no decrease in the total energy needed. Starting from 202 and 211 TWh/y at the optimums in cost and energy invested, the minimum amount of this type of energy is still around 174 TWh/y (i.e., −20% and −15% respectively) for deviations of 10%. Most of the decrease is already present for deviations of 1% with an amount of energy of 180 TWh/y, which is only 6 TWh/y less than the energy used at one of the efficient solutions. The $\tilde{c}$ value of non-implied necessary conditions then plateaus at 174 TWh/y. This result shows how, contrarily to endogenous resources, exogenous resources are essential, whatever the cost and energy invested. Indeed, to respect a GWP_{tot} constraint of 35 MtCO$_2$-eq/y, at least 174 TWh/y of energy needs to be imported.

4.3.2. Individual exogenous resources

We have shown that a certain amount of exogenous resources is necessary due to limited endogenous resources. However, the previous results do not show which specific exogenous resource is essential. This analysis can be done by computing necessary conditions for groups of conditions $\Phi_{\{i\}}$ where $i \in RES$ corresponds to a unique resource. We could perform this analysis for all individual resources, but in Fig. 6(b), the amounts of renewable methanol, gas, and imported electricity are quasi-constant across the Pareto front. Therefore, it is interesting to focus on these resources to see if they are essential or if we can eliminate them by increasing the cost or the invested energy. In this section, we analyse non-implied necessary conditions corresponding to the minimum energy from these three resources.

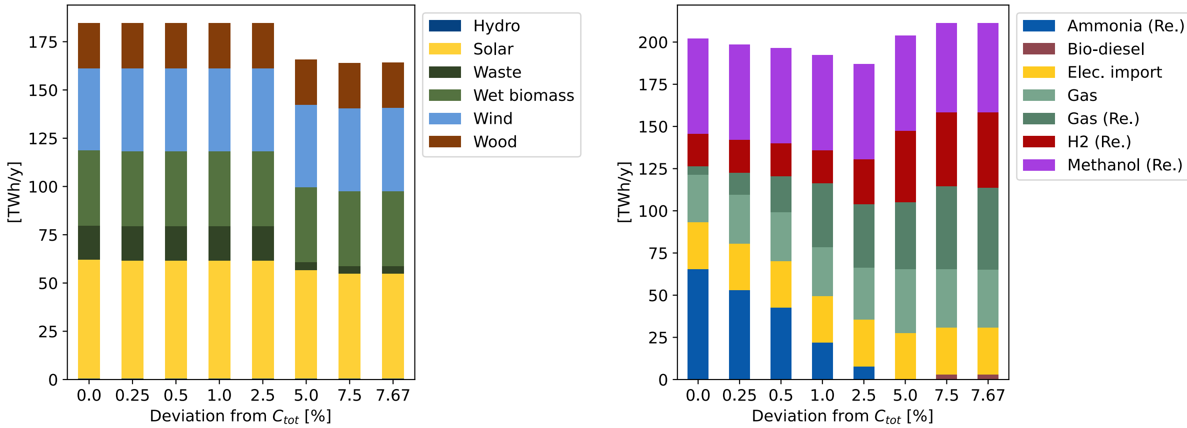

(a) Endogenous resources

(b) Exogenous resources

Fig. 6. Energy [TWh/y] coming from (a) endogenous and (b) exogenous resources at efficient solutions representing different trade-offs between C_{tot} and E_{in}. The leftmost bars show these values at the C_{tot} optimum, while the rightmost bar shows these values at the E_{in} optimum. The bars in the middle are characterised by their deviation in [%] from the C_{tot} optimum. Abbreviations: Renewable (Re.), Electricity (Elec.).

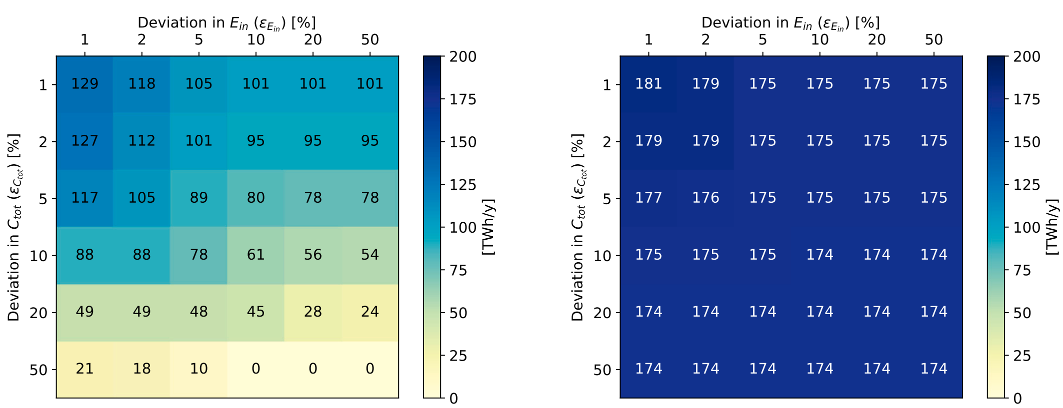

(a) Endogenous resources

(b) Exogenous resources

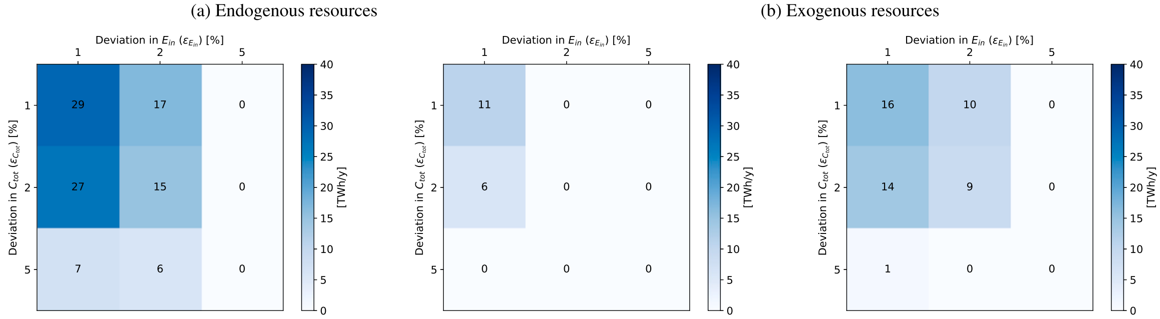

(c) Renewable methanol

(d) Gas

(e) Electricity import

Fig. 7. Values $\tilde{c}$ of necessary conditions (in [TWh/y]) for conditions of type $\Phi_{\overline{RES}}$. The set of resources $\overline{RES}$ corresponds to endogenous resources RES_{endo} and exogenous resources RES_{exo} for graph (a) and (b), respectively, while for graphs (c), (d) and (e), this set resumes to a single resource: renewable methanol, gas and imported electricity, respectively. The values correspond to the minimum amount of energy that needs to come from these sets of resources to ensure a constrained deviation in C_{tot} and E_{in}. These deviations are defined by the suboptimality coefficients vector $\epsilon = (\epsilon_{C_{tot}}, \epsilon_{E_{in}})$. For (a) and (b), all the combinations of the following percentages are taken as coefficients vectors: 1%, 2%, 5%, 10%, 20%, and 50%. For (c), (d) and (e), they are limited to the combinations of 1%, 2%, and 5%.

The $\tilde{c}$ values of non-implied necessary conditions for deviations $\epsilon_{C_{tot}}$ and $\epsilon_{E_{in}}$ of 1, 2 and 5% are shown in Figs. 7(c), 7(d), and 7(e). We limit the analysis to deviations of 5% as we can see that we are already equal (or near to) 0 TWh/y for all three resources at this percentage. The amount of energy coming from the resources at the C_{tot} and E_{in} optimums are respectively 56.4 and 52.8 TWh/y for renewable methanol, 28.2 and 34.5 for gas, and 27.6 (at both optima) for imported electricity. The minimum energy from each resource is around 50% lower than at the efficient solutions when allowing deviations of 1% in each objective. For renewable methanol and gas, the amount of necessary energy is more sensitive to deviations in invested energy than to deviations in cost. However, the conclusion is similar for the three resources: for a relatively small increase in cost and invested energy, they can be replaced by other resources.

4.4. Analysis and insights from the results

In response to the initial query of this case study, "Which endogenous or exogenous resources are necessary in Belgium to ensure a transition associated with sufficiently good cost and EROI?" our analysis offers multiple insights. Examination of the optimums for each objective revealed that endogenous resources are instrumental in achieving an attractive cost and EROI. It also highlighted that various exogenous resources could contribute to this outcome. Looking at points along the Pareto front, we then refined this analysis. This next step proved particularly informative for exogenous resources, revealing a spectrum of energy mixes satisfying reasonable cost and EROI trade-offs. Finally, the computation of necessary conditions unveiled an innovative perspective. Despite being maximised at the optimums, endogenous resources could be significantly reduced with relatively minor increases in cost and invested energy. Conversely, while numerous exogenous resource mixes offered a good cost and EROI, the total energy derived from these sources could not fall below a certain threshold. Necessary conditions also corroborated the broad range of exogenous mixes available, indicating that no specific resource is indispensable when accounting for a moderate relaxation of the objectives.

These findings suggest that for Belgium to decarbonise its economy, it must substantially rely on imported resources. This necessitates careful management of factors that can mitigate Belgium's dependence, such as enhancing energy efficiency, increasing land use for renewable energy production, and maintaining positive geopolitical relations with various providers. Fortunately, allowing for acceptable deviations in cost and EROI gives Belgium a wide choice in selecting imported energy sources, offering opportunities for diversification and a more reliable energy system.

While this analysis is specific to Belgium, similar considerations apply to other countries in the European Union, one of the most densely populated regions globally. Therefore, it is crucial to evaluate their dependence on exogenous resources and the potential trade-offs and opportunities.

5. Conclusion

The ongoing energy transition necessitates profound restructuring of energy systems over the long term. Energy system optimisation models (ESOMs) are critical in steering this restructuring and identifying the optimal blend of energy sources and technologies to meet future energy demand. However, focusing solely on cost when using these models limits the value of the insights they can provide decision-makers.

We address this issue by introducing a methodology for exploring the near-optimal spaces of multi-objective problems to answer specific socio-technical questions and applying it to a specific case study.

Building upon the research of Dubois and Ernst [23], we extend the principles of epsilon-optimality and non-implied necessary conditions to multi-objective problems. These concepts are applied to the case of Belgium's whole-energy system in 2035, with an emissions target below 35 $MtCO_2$/y, equating to an approximate 80% reduction compared to 2015 levels [38]. The case study involved identifying the necessary endogenous or exogenous resources to ensure a transition with reasonable cost and EROI. This need is determined by computing non-implied necessary conditions, representing the minimum energy amount derived from various resource sets to ensure a constrained deviation in cost and energy invested. Our research findings suggest that while Belgium could significantly curtail its consumption of endogenous resources, diminishing reliance on exogenous resources presents a complex challenge. Furthermore, our results underscore the versatility of potential exogenous resources.

The current methodology encounters a set of limitations that, if addressed, could enhance the reliability of the results. The primary constraint relates to the approximation of the epsilon-optimal space in multi-objective optimisation problems, which affects the identification of non-implied necessary conditions. Increasing the number of efficient solutions can improve results but amplifies computational time. To mitigate this constraint, future research could examine the influence of the number and distribution of efficient solutions on the findings. Another consideration involves the visual presentation of the results. Specifically, necessary conditions for constrained deviations in two objectives can be effectively displayed on a two-dimensional grid. However, should the objectives exceed two, or if near-optimal space analysis is merged with parametric uncertainty analysis, new innovative techniques will be required to encapsulate the results succinctly.

Potential avenues for future research could contribute to expanding the current methodology. Firstly, the method was developed around the concept of necessary conditions. However, other methodologies were developed to explore near-optimal spaces in a mono-objective setup as presented, for instance, in Price and Keppo [18], Li and Trutnevyte [19], Pedersen et al. [20] and Nacken et al. [52]. An interesting research track would be to extend these methodologies in a multi-objective setup. Secondly, the current methodology was developed for fixed feasible spaces and objective functions. Incorporating techniques for addressing parametric uncertainty, such as sensitivity analysis, would enhance the breadth and applicability of the results.

Lastly, extensive research is required to substantiate the utility of the method across varied contexts. Future research could replicate the case study for different nations or regions grappling with resource constraints and challenges of energy dependence. Moreover, while cost and invested energy were the primary objectives in this study, other criteria like land use, water use, or metal resources could be explored. This framework could also be utilised to answer alternative queries about various resources or technologies. Ultimately, this approach could be extended to study near-optimal spaces for various optimisation problems within and beyond the energy systems field.

CRediT authorship contribution statement

Antoine Dubois: Conceptualization, Methodology, Software, Validation, Formal analysis, Investigation, Data curation, Writing – original draft, Writing – review & editing. **Jonathan Dumas:** Conceptualization, Software, Data curation, Writing – review & editing, Supervision. **Paolo Thiran:** Conceptualization, Software, Writing – review & editing. **Gauthier Limpens:** Conceptualization, Software, Data curation, Writing – review & editing, Supervision. **Damien Ernst:** Conceptualization, Methodology, Writing – review & editing, Supervision.

Declaration of competing interest

The authors declare that they have no known competing financial interests or personal relationships that could have appeared to influence the work reported in this paper.

Data availability

The data is available on a open repository: https://zenodo.org/record/7665340.

Declaration of Generative AI and AI-assisted technologies in the writing process

During the preparation of this work, the author(s) used ChatGPT in order to improve the formulation of certain sections. After using this tool/service, the author(s) reviewed and edited the content as needed and take(s) full responsibility for the content of the publication.

Acknowledgements

Antoine Dubois is a Research Fellow of the F.R.S.-FNRS, of which he acknowledges the financial support.

Appendix A. Numerical values of the epsilon-space examples

The functions depicted in Figs. 2, 3, and 4 are

$$f_1(x) = 10 * (2x - 0.75)^2 + 2 \quad \text{and} \tag{A.1}$$

$$f_2(x) = 10 * (x - 0.75)^2 + 1.5 \quad . \tag{A.2}$$

The coordinates of their minimums are $(x_1^*, f_1(x_1^*)) = (0.375, 2)$ and $(x_2^*, f_2(x_2^*)) = (0.75, 1.5)$, respectively.

One-dimensional epsilon-optimal space

In Fig. 2, the ϵ-optimal space $\mathcal{X}^\epsilon$ of a one-dimensional optimisation problem was obtained by first computing

$$(1 + \epsilon_1) f_1(x_1^*) = (1 + 0.25) * 2 = 2.5 \tag{A.3}$$

where $\epsilon_1 = 0.25$. Then, the limits of $\mathcal{X}^\epsilon$ can be obtained by computing the inverse image of this value, i.e. the set $\{0.263, 0.487\}$, which leads to $\mathcal{X}^\epsilon = [0.263, 0.487]$.

Two-dimensional epsilon-optimal space

In Figs. 3(a) and 3(b), the Pareto front $\mathcal{P}_\mathcal{X}$ is represented in green. This set of points respects Definition 6 of a Pareto front. Indeed, each point x in the interval $[x_1^\star, x_2^\star]$ is such that $\nexists \hat{x} \in \mathcal{X}$ where $f_1(\hat{x}) < f_1(x)$ and $f_2(\hat{x}) < f_2(x)$.

In Fig. 3(b), a subset of the ϵ-optimal space $\mathcal{X}^\epsilon$ of a two-dimensional optimisation problem is computed for a suboptimality coefficients vector $\boldsymbol{\epsilon} = (\epsilon_1, \epsilon_2) = (0.25, 0.6)$. This subset is computed from the point $\hat{x} = 0.6$, which is part of $\mathcal{P}_\mathcal{X}$. To obtain the subset of $\mathcal{X}^\epsilon$, the images of $\hat{x}$, $f_1(\hat{x}) = 4.025$ and $f_2(\hat{x}) = 1.725$, are computed. Multiplying these values by the corresponding suboptimality coefficients gives

$$(1 + \epsilon_1) f_1(\hat{x}) = (1 + 0.25) * 4.025 = 5.03 \quad \text{and} \tag{A.4}$$

$$(1 + \epsilon_2) f_2(\hat{x}) = (1 + 0.6) * 1.725 = 2.76 \quad . \tag{A.5}$$

The inverse image of these values are $\{0.0997, 0.65\}$ for f_1 and $\{0.395, 1.105\}$ for f_2. The set of points respecting $\forall k\ f_k(x) \leq (1+\epsilon_k) f_k(\hat{x})$ are then contained in $[0.395, 0.65]$.

To obtain the full ϵ-optimal space depicted in Fig. 3(a), one should repeat this process with all points in $\mathcal{P}_\mathcal{X}$. However, in this simple example, one can quickly compute the limits of the entire space by using the two optimums, which are the extreme points of the Pareto front. These limits are obtained by taking the inverse images of

$$(1 + \epsilon_1) f_1(x_1^*) = (1 + 0.25) * 2 = 2.5 \quad \text{and} \tag{A.6}$$

$$(1 + \epsilon_2) f_2(x_2^*) = (1 + 0.6) * 1.5 = 2.4 \quad , \tag{A.7}$$

which gives $\{0.263, 0.487\}$ and $\{0.45, 1.05\}$. The lower and upper bound of $\mathcal{X}^\epsilon$ are then respectively given by the lower and upper bound of those two sets, i.e. $\mathcal{X}^\epsilon = [0.263, 1.05]$.

Approximate Pareto fronts and epsilon-optimal spaces

Figs. 4(a), 4(b), and 4(c) show approximate $\boldsymbol{\epsilon}$-optimal spaces for three different set of efficient points. These sets are

1. Fig. 4(a): [(2.0, 2.91), (3.41, 1.85), (7.62, 1.5)];
2. Fig. 4(b): [(2.9, 2.01), (2.99, 1.97), (3.09, 1.94), (3.19, 1.91), (3.3, 1.88), (3.41, 1.85), (3.52, 1.82), (3.64, 1.8), (3.77, 1.77), (3.9, 1.75), (4.03, 1.72)];
3. Fig. 4(c): [(2.0, 2.91), (2.06, 2.64), (2.23, 2.40), (2.51, 2.19), (2.9, 2.01), (3.41, 1.85), (4.03, 1.72), (4.76, 1.63), (5.61, 1.56), (6.57, 1.51), (7.62, 1.5)].

Appendix B. Necessary conditions - Advanced definitions

B.1. Implication

The *implication* between two conditions can be defined mathematically and allow for a more formal definition of non-implied necessary conditions.

Definition 10. An **implication function** $\psi(\phi_1 \mid \phi_2) \in \{0, 1\}$ is a function that indicates whether condition ϕ_2 implies condition ϕ_1. When $\psi(\phi_1 \mid \phi_2) = 1$, then $\forall x \in \mathcal{X},\ \phi_2(x) = 1 \implies \phi_1(x) = 1$. When $\psi(\phi_1 \mid \phi_2) = 0$, then $\exists x \in \mathcal{X},\ \phi_2(x) = 1 \not\Longrightarrow \phi_1(x) = 1$.

Example. Let us consider conditions $\phi_1(x) := x \geq 1$ and $\phi_2(x) := x \geq 2$ of the example introduced in Section 2.1.2. We have that $\psi(\phi_1 \mid \phi_2) = 1$. Indeed, for all $x \in \mathcal{X}$, if $\phi_2(x) = 1$ this means that $x \geq 2$, that $x \geq 1$ and thus $\phi_1(x) = 1$. Conversely, $\psi(\phi_2 \mid \phi_1) = 0$. Indeed, there exist several $x \in \mathcal{X}$ such that $\phi_1(x) = 1$ and $\phi_2(x) = 0$. For instance, this is the case for $x = 1.5$.

Definition 11. A **non-implied necessary condition** is a necessary condition $\phi \in \Phi^{\mathcal{X}^\epsilon}$ that is not implied by any other necessary condition. It is a necessary condition $\phi \in \Phi^{\mathcal{X}^\epsilon}$ such that $\forall \phi' \in \Phi^{\mathcal{X}^\epsilon} \setminus \{\phi\} : \psi(\phi \mid \phi') = 0$.

Example. The condition ϕ_0 respects this definition. Indeed, for any other condition $\phi' \in \Phi^{\mathcal{X}^\epsilon}$, that is any ϕ_c with $c < 0$, we have $\psi(\phi_0 \mid \phi_c) = 0$. The proof is straightforward. For any $c < 0$, $\phi_c(c) = 1$ as $c \geq c$ is true, but $\phi_0(c) = 0$ as $c \geq 0$ is false.

B.2. Necessary conditions - True spaces

A last way to particularise the definition of (non-implied) necessary conditions is by defining the space over which a condition is true.

Definition 12. The space $\mathcal{I}_\phi$ is the subset of $\mathcal{X}$ where a condition ϕ is true, that is:

$$\mathcal{I}_\phi = \left\{ x \in \mathcal{X} \mid \phi(x) = 1 \right\} \quad . \tag{B.1}$$

Example. The spaces $\mathcal{I}_{\phi_c}$ of the conditions $\phi_c(x) := x \geq c$ are the spaces $[c, \infty]$. These spaces might become more complex to determine when considering, for instance, conditions using linear combinations of variables, e.g. $\phi(x) := ax_1 + bx_2 \geq c$ with $x = (x_1, x_2) \in \mathcal{X} = \mathbb{R}^2$.

Definition 13. A **necessary condition** for ϵ-optimality is a condition ϕ such that $\mathcal{X}_\epsilon \subseteq \mathcal{I}_\phi$.

Example. For a set of conditions $\Phi = \{\phi_c(x) := x \geq c\}$ with $x \in \mathbb{R}$ and $c \in \mathbb{R}$, and a ϵ-optimal space $\mathcal{X}^\epsilon = [0, 1]$, this definition implies that all conditions ϕ_c with $c \leq 0$ are necessary, which corresponds to same set as Definition 3. Indeed, the spaces $\mathcal{I}_{\phi_c} = [c, \infty]$ include the space $[0, 1]$, when $c \leq 0$.

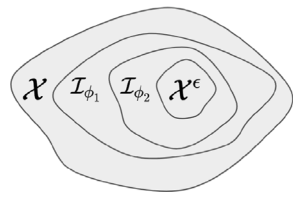

Fig. B.8. Graphical illustration of implication using spaces over which conditions are true, adapted from Dubois and Ernst [23]. The four spaces that are represented are the feasible space $\mathcal{X}$, the ϵ-optimal space $\mathcal{X}^\epsilon$, and the spaces $\mathcal{I}_{\phi_1}$ and $\mathcal{I}_{\phi_2}$ where conditions ϕ_1 and ϕ_2 are respectively true. Both these conditions are necessary as $\mathcal{X}^\epsilon \subset \mathcal{I}_{\phi_1}$ and $\mathcal{X}^\epsilon \subset \mathcal{I}_{\phi_2}$. Moreover, ϕ_2 implies ϕ_1 as $\mathcal{I}_{\phi_2} \subset \mathcal{I}_{\phi_1}$.

Table C.5
2035 Belgian end-use demand (EUD) value by type based on Limpens [53]. Abbreviations: temperature (T.), space heating (SP), hot water (HW), passenger (pass.).

EUD type	Unit	EUD
Electricity (other)	TWhe	62.1
Lighting	TWhe	30.0
Heat high T.	TWh	50.4
Heat low T. (SH)	TWh	118
Heat low T. (HW)	TWh	29.2
Passenger mobility	Mpass.-km	194
Freight	Mt-km	98.0
Non-energy	TWh	53.1

Definition 14. Let ϕ_1 and ϕ_2 be conditions with $\mathcal{I}_{\phi_1}$ and $\mathcal{I}_{\phi_2}$ the spaces over which they are respectively true, then the **implication function** $\psi(\phi_1 \mid \phi_2)$ is defined as:

$$\psi(\phi_1 \mid \phi_2) = \mathcal{I}_{\phi_2} \subseteq \mathcal{I}_{\phi_1} \quad . \tag{B.2}$$

This formulation fits Definition 10 of an implication function. Indeed, if $\psi(\phi_1 \mid \phi_2) = 1$, then it means $\mathcal{I}_{\phi_2} \subseteq \mathcal{I}_{\phi_1}$, which in turns implies that $\phi_1(x) = 1$ for any $x \in \mathcal{X}$ for which $\phi_2(x) = 1$. Similarly, if $\psi(\phi_1 \mid \phi_2) = 0$, it means that $\mathcal{I}_{\phi_2} \nsubseteq \mathcal{I}_{\phi_1}$, which means $\exists x \in \mathcal{X}$ such that $\phi_1(x) = 0$ when $\phi_2(x) = 1$.

Definition 15. A **non-implied necessary condition** is a necessary condition $\phi \in \Phi^{\mathcal{X}^\epsilon}$ that is true over a space which does not include any of the spaces over which other necessary conditions are true. It is a necessary condition $\phi \in \Phi^{\mathcal{X}^\epsilon}$ such that $\forall \phi' \in \Phi^{\mathcal{X}^\epsilon} \setminus \{\phi\} : \mathcal{I}_{\phi'} \nsubseteq \mathcal{I}_{\phi}$.

Fig. B.8 illustrates these concepts, where ϕ_2 implies ϕ_1 as $\mathcal{I}_{\phi_2} \subset \mathcal{I}_{\phi_1}$. They are both necessary conditions because they are true over $\mathcal{X}^\epsilon$. Finally, if no other conditions exist in the set $\Phi = \{\phi_1, \phi_2\}$, then ϕ_2 is a non-implied necessary condition as no other necessary condition implies it.

Appendix C. Types of end-use demand in EnergyScope-TD

Four main types of EUD are considered in the model: electricity, heat, transport, and non-energy demand. Electricity is further divided between lighting and other electricity uses. Heat is subdivided into high-temperature heat for industry, low temperature for space heating, and low temperature for hot water. Mobility is composed of public and private passenger mobility and freight demands. Finally, the non-energy demand includes demand for ammonia, methanol, and high-value chemicals (HVCs). Table C.5 lists the values for each EUD type in 2035 based on Limpens [53].

Appendix D. Computation of non-implied necessary conditions for the case study

Algorithm 3 is an adapted version of Algorithm 2 allowing to compute a non-implied necessary condition for a fixed set of resources $\overline{RES}$ and suboptimality coefficients vector $\boldsymbol{\epsilon}$.

Algorithm 3: Computation of one non-implied necessary condition for a given set of resources and suboptimality coefficients vector. Adaptation of Algorithm 2 to the case study.

Data:
$\mathcal{X} \in \mathbb{R}^n$ - feasible space defined via ESTD,
$\mathbf{f} = (C_{tot}, E_{in})$,
m - number of points,
$\boldsymbol{\epsilon} = (\epsilon_{C_{tot}}, \epsilon_{E_{in}})$,
$\overline{RES}$ - a set of resources

Result: $\tilde{c}$

Steps:

1. Compute the two optimums $C^\star_{tot} = \arg\min_{\mathcal{X}} C_{tot}$ and $E^\star_{in} = \arg\min_{\mathcal{X}} E_{in}$ (and derive C^e_{tot}, i.e. the value of C_{tot} at the E_{in} optimum).
2. Apply method (23) for $m-2$ values of ϵ in $]0, C^e_{tot}/C^\star_{tot}[$ to obtain points $\hat{\mathbf{x}}^{(2)}, \dots \hat{\mathbf{x}}^{(j)}, \dots \hat{\mathbf{x}}^{(m-1)}$ of the Pareto front. Points $\hat{\mathbf{x}}^{(1)}$ and $\hat{\mathbf{x}}^{(m)}$ correspond to the C_{tot} and E_{in} optimums, respectively.
3. For all $j \in [1, 2, \dots, m]$, compute

$$c^{(j)} = \min \sum_{\substack{i \in \overline{RES}, \\ t \in T \mid \{h,td\} \in THTD(t)}} \mathbf{F}_t(i, h, td) \tag{D.1}$$

over the space

$$\{\mathbf{x} \in \mathcal{X} \mid C_{tot}(\mathbf{x}) \le (1 + \epsilon_{C_{tot}}) C_{tot}(\hat{\mathbf{x}}^{(j)}), \quad E_{in}(\mathbf{x}) \le (1 + \epsilon_{E_{in}}) E_{in}(\hat{\mathbf{x}}^{(j)})\}, \tag{D.2}$$

where $C_{tot}(\mathbf{x})$ and $E_{in}(\mathbf{x})$ represent the values of the two objectives at solution $\mathbf{x}$.

4. Take the minimum $\tilde{c} = \min_{j \in [1,2,\dots,m]} c^{(j)}$ to find the non-implied necessary condition:

$$\phi_{\tilde{c}} = \sum_{\substack{i \in \overline{RES}, \\ t \in T \mid \{h,td\} \in THTD(t)}} \mathbf{F}_t(i, h, td) \ge \tilde{c} \quad , \tag{D.3}$$

References

[1] DeCarolis J, Daly H, Dodds P, Keppo I, Li F, McDowall W, Pye S, Strachan N, Trutnevyte E, Usher W, Winning M, Yeh S, Zeyringer M. Formalizing best practice for energy system optimization modelling. Appl Energy 2017;194:184–98. http://dx.doi.org/10.1016/j.apenergy.2017.03.001.

[2] Pfenninger S, Hawkes A, Keirstead J. Energy systems modeling for twenty-first century energy challenges. Renew Sustain Energy Rev 2014;33:74–86. http://dx.doi.org/10.1016/j.rser.2014.02.003.

[3] Fishbone LG, Abilock H. MARKAL, a linear-programming model for energy systems analysis: Technical description of the BNL version. Int J Energy Res 1981;5(4):353–75. http://dx.doi.org/10.1002/er.4440050406.

[4] Schrattenholzer L. The energy supply model MESSAGE. 1981, URL https://pure.iiasa.ac.at/id/eprint/1542/.

[5] Quoilin S, Hidalgo Gonzalez I, Zucker A. Modelling future EU power systems under high shares of renewables: The Dispa-SET 2.1 open-source model. 2017, URL https://orbi.uliege.be/handle/2268/205771.

[6] Yue X, Pye S, DeCarolis J, Li FG, Rogan F, Gallachóir BÓ. A review of approaches to uncertainty assessment in energy system optimization models. Energy Strategy Rev 2018;21:204–17. http://dx.doi.org/10.1016/j.esr.2018.06.003.

[7] Fazlollahi S, Mandel P, Becker G, Maréchal F. Methods for multi-objective investment and operating optimization of complex energy systems. Energy 2012;45(1):12–22. http://dx.doi.org/10.1016/j.energy.2012.02.046.

[8] Trutnevyte E. Does cost optimization approximate the real-world energy transition? Energy 2016;106:182–93. http://dx.doi.org/10.1016/j.energy.2016.03.038.

[9] Fujino J, Hibino G, Ehara T, Matsuoka Y, Masui T, Kainuma M. Back-casting analysis for 70% emission reduction in Japan by 2050. Clim Policy 2008;8(sup1):S108–24. http://dx.doi.org/10.3763/cpol.2007.0491.

[10] Hughes N, Strachan N. Methodological review of UK and international low carbon scenarios. Energy Policy 2010;38(10):6056–65. http://dx.doi.org/10.1016/j.enpol.2010.05.061.

[11] Becerra-López HR, Golding P. Multi-objective optimization for capacity expansion of regional power-generation systems: Case study of far west Texas. Energy Convers Manage 2008;49(6):1433–45. http://dx.doi.org/10.1016/j.enconman.2007.12.021.

[12] Fonseca JD, Commenge J-M, Camargo M, Falk L, Gil ID. Multi-criteria optimization for the design and operation of distributed energy systems considering sustainability dimensions. Energy 2021;214:118989. http://dx.doi.org/10.1016/j.energy.2020.118989.

[13] Fonseca JD, Commenge J-M, Camargo M, Falk L, Gil ID. Sustainability analysis for the design of distributed energy systems: A multi-objective optimization approach. Appl Energy 2021;290:116746. http://dx.doi.org/10.1016/j.apenergy.2021.116746.

[14] Jing R, Zhu X, Zhu Z, Wang W, Meng C, Shah N, Li N, Zhao Y. A multi-objective optimization and multi-criteria evaluation integrated framework for distributed energy system optimal planning. Energy Convers Manage 2018;166:445–62. http://dx.doi.org/10.1016/j.enconman.2018.04.054.

[15] DeCarolis JF. Using modeling to generate alternatives (MGA) to expand our thinking on energy futures. Energy Econ 2011;33(2):145–52. http://dx.doi.org/10.1016/j.eneco.2010.05.002.

[16] Brill ED, Chang S-Y, Hopkins LD. Modeling to generate alternatives: The HSJ approach and an illustration using a problem in land use planning. Manage Sci 1982;28(3):221–35. http://dx.doi.org/10.1287/mnsc.28.3.221.

[17] DeCarolis J, Babaee S, Li B, Kanungo S. Modelling to generate alternatives with an energy system optimization model. Environ Model Softw 2016;79:300–10. http://dx.doi.org/10.1016/j.envsoft.2015.11.019.

[18] Price J, Keppo I. Modelling to generate alternatives: A technique to explore uncertainty in energy-environment-economy models. Appl Energy 2017;195:356–69. http://dx.doi.org/10.1016/j.apenergy.2017.03.065.

[19] Li FG, Trutnevyte E. Investment appraisal of cost-optimal and near-optimal pathways for the UK electricity sector transition to 2050. Appl Energy 2017;189:89–109. http://dx.doi.org/10.1016/j.apenergy.2016.12.047.

[20] Pedersen TT, Victoria M, Rasmussen MG, Andresen GB. Modeling all alternative solutions for highly renewable energy systems. Energy 2021;121294. http://dx.doi.org/10.1016/j.energy.2021.121294.

[21] Grochowicz A, van Greevenbroek K, Benth FE, Zeyringer M. Intersecting near-optimal spaces: European power systems with more resilience to weather variability. Energy Econ 2023;118:106496. http://dx.doi.org/10.1016/j.eneco.2022.106496.

[22] Neumann F, Brown T. The near-optimal feasible space of a renewable power system model. Electr Power Syst Res 2021;190:106690. http://dx.doi.org/10.1016/j.epsr.2020.106690.

[23] Dubois A, Ernst D. Computing necessary conditions for near-optimality in capacity expansion planning problems. Electr Power Syst Res 2022;211:108343. http://dx.doi.org/10.1016/j.epsr.2022.108343.

[24] Dubois A, Dumas J, Limpens G, Thiran P. Multi-objective near-optimal necessary conditions for multi-sectoral planning - code. 2023, http://dx.doi.org/10.5281/zenodo.7665440.

[25] Dubois A, Dumas J, Limpens G, Thiran P. Multi-objective near-optimal necessary conditions for multi-sectoral planning - dataset. 2023, http://dx.doi.org/10.5281/zenodo.7665340.

[26] Ehrgott M. Multicriteria optimization. vol. 491, Springer Science & Business Media; 2005, http://dx.doi.org/10.1007/978-3-662-22199-0.

[27] Alarcon-Rodriguez A, Ault G, Galloway S. Multi-objective planning of distributed energy resources: A review of the state-of-the-art. Renew Sustain Energy Rev 2010;14(5):1353–66. http://dx.doi.org/10.1016/j.rser.2010.01.006.

[28] European Commission. European Green Deal. 2021, URL https://ec.europa.eu/clima/eu-action/european-green-deal_en, [accessed 08-June-2022].

[29] International Energy Agency. IEA - Energy Statistics Data Browser. 2022, URL https://www.iea.org/data-and-statistics/data-tools/energy-statistics-data-browser, [accessed 17-June-2022].

[30] Commission E, for Climate Action D-G, for Energy D-G, for Mobility D-G, Transport, Zampara M, Obersteiner M, Evangelopoulou S, De Vita A, Winiwarter W, Witzke H, Tsani S, Kesting M, Paroussos L, Höglund-Isaksson L, Papadopoulos D, Capros P, Kannavou M, Siskos P, Tasios N, Kouvaritakis N, Karkatsoulis P, Fragkos P, Gomez-Sanabria A, Petropoulos A, Havlík P, Frank S, Purohit P, Fragiadakis K, Forsell N, Gusti M, Nakos C. EU reference scenario 2016 : energy, transport and GHG emissions : trends to 2050. Publications Office; 2016, http://dx.doi.org/10.2833/001137.

[31] Dupont E, Germain M, Jeanmart H. Estimate of the societal energy return on investment (EROI). Biophys Econ Sustain 2021;6(1):1–14. http://dx.doi.org/10.1007/s41247-021-00084-9.

[32] Brockway PE, Owen A, Brand-Correa LI, Hardt L. Estimation of global final-stage energy-return-on-investment for fossil fuels with comparison to renewable energy sources. Nat Energy 2019;4(7):612–21. http://dx.doi.org/10.1038/s41560-019-0425-z.

[33] Dumas J, Dubois A, Thiran P, Jacques P, Contino F, Cornélusse B, Limpens G. The energy return on investment of whole-energy systems: Application to Belgium. Biophys Econ Sustain 2022;7(4):12. http://dx.doi.org/10.1007/s41247-022-00106-0.

[34] European Commission - Eurostat. Glossary: Final Energy Consumption. 2022, URL https://ec.europa.eu/eurostat/statistics-explained/index.php?title=Glossary:Final_energy_consumption, [accessed 17-June-2022].

[35] Khattabi Z. Press release - 8 Octobre 2021. 2021, URL https://khattabi.belgium.be/, [accessed 26-Jul-2022].

[36] European Commission - Eurostat. Eurostat - Population density. 2022, URL https://ec.europa.eu/eurostat/databrowser/view/tps00003/default/table, [accessed 17-June-2022].

[37] Belgian Offshore Platform. Belgian Offshore Platform. 2022, URL https://www.belgianoffshoreplatform.be/en/, [accessed 26-Jul-2022].

[38] Limpens G, Jeanmart H, Maréchal F. Belgian energy transition: What are the options? Energies 2020;13(1). http://dx.doi.org/10.3390/en13010261.

[39] Limpens G, Moret S, Jeanmart H, Maréchal F. EnergyScope TD: A novel open-source model for regional energy systems. Appl Energy 2019;255:113729. http://dx.doi.org/10.1016/j.apenergy.2019.113729.

[40] Contino F, Moret S, Limpens G, Jeanmart H. Whole-energy system models: The advisors for the energy transition. Prog Energy Combust Sci 2020;81:100872. http://dx.doi.org/10.1016/j.pecs.2020.100872.

[41] Limpens G, Coppitters D, Rixhon X, Contino F, Jeanmart H. The impact of uncertainties on the belgian energy system: Application of the polynomial chaos expansion to the energyscope model. In: ECOS 2020 - proceedings of the 33rd international conference on efficiency, cost, optimization, simulation and environmental impact of energy systems. 2020, p. 724–33, URL http://hdl.handle.net/2078.1/231513.

[42] Rixhon X, Limpens G, Coppitters D, Jeanmart H, Contino F. The role of electrofuels under uncertainties for the belgian energy transition. Energies 2021;14(13). http://dx.doi.org/10.3390/en14134027.

[43] Colla M, Blondeau J, Jeanmart H. Optimal use of lignocellulosic biomass for the energy transition, including the non-energy demand: The case of the belgian energy system. Front Energy Res 2022;10. http://dx.doi.org/10.3389/fenrg.2022.802327.

[44] Limpens G, Jeanmart H. System LCOE: Applying a whole-energy system model to estimate the integration costs of photovoltaic. In: Proceedings of the ECOS2021—the 34th international conference, Taormina, Italy, June. 2021, p. 28–2, URL http://hdl.handle.net/2078.1/252944.

[45] Li X, Damartzis T, Stadler Z, Moret S, Meier B, Friedl M, Maréchal F. Decarbonization in complex energy systems: A study on the feasibility of carbon neutrality for Switzerland in 2050. Front Energy Res 2020;8. http://dx.doi.org/10.3389/fenrg.2020.549615.

[46] Guevara E, Babonneau F, de Mello TH, Moret S. A machine learning and distributionally robust optimization framework for strategic energy planning under uncertainty. Appl Energy 2020;271:115005. http://dx.doi.org/10.1016/j.apenergy.2020.115005.

[47] Borasio M, Moret S. Deep decarbonisation of regional energy systems: A novel modelling approach and its application to the Italian energy transition. Renew Sustain Energy Rev 2022;153:111730. http://dx.doi.org/10.1016/j.rser.2021.111730.

[48] Limpens G. EnergyScope TD Documentation. 2022, URL https://energyscope.readthedocs.io/en/master/, [accessed 07-May-2023].

[49] Muyldermans B, Nève G. Multi-criteria optimisation of an energy system and application to the Belgian case Master's thesis, UCL - Ecole polytechnique de Louvain; 2021, URL http://hdl.handle.net/2078.1/thesis:33139.

[50] Wernet G, Bauer C, Steubing B, Reinhard J, Moreno-Ruiz E, Weidema B. The ecoinvent database version 3 (part i): overview and methodology. Int J Life Cycl Assess 2016;21(9):1218–30. http://dx.doi.org/10.1007/s11367-016-1087-8.

[51] Orban A. Energy return on investment of electrofuels Master's thesis, ULiège; 2022, URL https://matheo.uliege.be/handle/2268.2/15914.

[52] Nacken L, Krebs F, Fischer T, Hoffmann C. Integrated renewable energy systems for Germany–A model-based exploration of the decision space. In: 2019 16th International Conference on the European Energy Market. EEM, IEEE; 2019, p. 1–8. http://dx.doi.org/10.1109/EEM.2019.8916442.

[53] Limpens G. Generating energy transition pathways: application to Belgium (Ph.D. thesis), UCL-Université Catholique de Louvain; 2021, URL http://hdl.handle.net/2078.1/249196.